Article

Cell Chemical Biology

Global Cysteine-Reactivity Profiling during Impaired Insulin/IGF-1 Signaling in *C. elegans* Identifies Uncharacterized Mediators of Longevity

Graphical Abstract

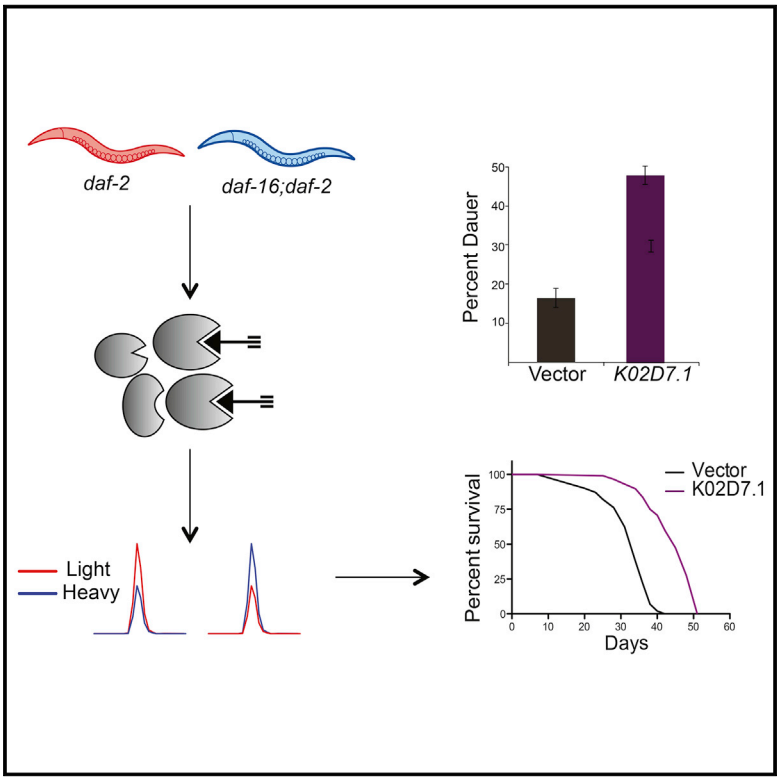

Authors

Julianne Martell, Yonghak Seo, Daniel W. Bak, Samuel F. Kingsley, Heidi A. Tissenbaum, Eranthie Weerapana

Correspondence

eranthie@bc.edu

In Brief

Martell et al. apply a reactive cysteine-profiling strategy to identify cysteine-mediated protein activity changes regulated by insulin/IGF-1 signaling. RNAi-mediated knockdown identified *lbp-3* and *K02D7.1* as novel mediators of *C. elegans* lifespan and dauer formation.

Highlights

- Hyperreactive and functional cysteines were identified in *C. elegans* lysates
- Comparing *daf-2* and *daf-16*;*daf-2* mutants revealed 40 proteins with >2-fold change
- RNAi-mediated knockdown characterized *lbp-3* and *K02D7.1* as regulators of lifespan
- These lifespan regulators are involved in fatty acid transport and purine metabolism

Martell et al., 2016, Cell Chemical Biology *23*, 1–12
August 18, 2016
http://dx.doi.org/10.1016/j.chembiol.2016.06.015

CellPress

Please cite this article in press as: Martell et al., Global Cysteine-Reactivity Profiling during Impaired Insulin/IGF-1 Signaling in *C. elegans* Identifies Uncharacterized Mediators of Longevity, Cell Chemical Biology (2016), http://dx.doi.org/10.1016/j.chembiol.2016.06.015

Cell Chemical Biology
Article

Global Cysteine-Reactivity Profiling during Impaired Insulin/IGF-1 Signaling in *C. elegans* Identifies Uncharacterized Mediators of Longevity

Julianne Martell,[1] Yonghak Seo,[2] Daniel W. Bak,[1] Samuel F. Kingsley,[2] Heidi A. Tissenbaum,[2,3] and Eranthie Weerapana[1,4,*]
[1]Department of Chemistry, Boston College, Chestnut Hill, MA 02467, USA
[2]Department of Molecular, Cell and Cancer Biology
[3]Program in Molecular Medicine
University of Massachusetts Medical School, Worcester, MA 01605, USA
[4]Lead Contact
*Correspondence: eranthie@bc.edu
http://dx.doi.org/10.1016/j.chembiol.2016.06.015

SUMMARY

In the nematode *Caenorhabditis elegans*, inactivating mutations in the insulin/IGF-1 receptor, DAF-2, result in a 2-fold increase in lifespan mediated by DAF-16, a FOXO-family transcription factor. Downstream protein activities that directly regulate longevity during impaired insulin/IGF-1 signaling (IIS) are poorly characterized. Here, we use global cysteine-reactivity profiling to identify protein activity changes during impaired IIS. Upon confirming that cysteine reactivity is a good predictor of functionality in *C. elegans*, we profiled cysteine-reactivity changes between *daf-2* and *daf-16;daf-2* mutants, and identified 40 proteins that display a >2-fold change. Subsequent RNAi-mediated knockdown studies revealed that *lbp-3* and *K02D7.1* knockdown caused significant increases in lifespan and dauer formation. The proteins encoded by these two genes, LBP-3 and K02D7.1, are implicated in intracellular fatty acid transport and purine metabolism, respectively. These studies demonstrate that cysteine-reactivity profiling can be complementary to abundance-based transcriptomic and proteomic studies, serving to identify uncharacterized mediators of *C. elegans* longevity.

INTRODUCTION

The insulin/insulin-like growth factor (IGF) signaling (IIS) pathway has been shown to modulate lifespan across phylogeny. The life-extending properties of impaired IIS have been observed in organisms including *Saccharomyces cerevisiae*, *Caenorhabditis elegans*, *Drosophila melanogaster*, and mice (reviewed in Barbieri et al., 2003). Furthermore, studies in humans revealed that genetic variations within components of the IIS pathway, in particular FOXO3A, were strongly associated with longevity (Anselmi et al., 2009; Flachsbart et al., 2009; Li et al., 2009; Willcox et al., 2008), implicating the IIS pathway as a common mediator of lifespan in both invertebrates and vertebrates.

C. elegans provides an ideal model organism for investigating the mechanistic basis of lifespan regulation due to its short and relatively invariant lifespan, enabling rapid evaluation of genetic and environmental factors that affect longevity (Olsen et al., 2006). In *C. elegans*, the IIS pathway is initiated by activation of the single insulin/IGF-1-like tyrosine kinase receptor, DAF-2, which results in phosphorylation and activation of a series of downstream protein kinases including phosphoinositide 3-kinase (PI3K; AGE-1), 3-phosphoinositide-dependent protein kinase-1 (PDK-1), and AKT/protein kinase B (PKB). AKT/PKB phosphorylation ultimately results in inactivation of a forkhead box O (FOXO) transcription factor, DAF-16 (Mukhopadhyay et al., 2006). Inactivation of DAF-2, or other kinases in the IIS pathway, results in DAF-16 translocation to the nucleus where DAF-16 targets genes that mediate IIS-regulated processes including longevity, fat storage, stress resistance, and dauer formation (Jensen et al., 2006; Oh et al., 2006; Lee et al., 2001; Lin et al., 2001; Henderson and Johnson, 2001). Dauer formation is a well-characterized alternative developmental pathway triggered by unfavorable growth conditions. Growth-arrested dauer larvae exhibit increased stress resistance, altered metabolism, increased longevity, and have the ability to survive without food for several months (Riddle et al., 1997). Many of the components of the IIS pathway were originally identified in genetic screens for genes that modulate dauer formation (Kenyon et al., 1993). Therefore, reduction-of-function mutations in genes in the IIS pathway, such as *daf-16* and *daf-2*, also modulate dauer diapause.

Inactivating mutations in the *C. elegans daf-2* gene results in a 2.3-fold increase in lifespan compared with wild-type (WT) animals (Kenyon et al., 1993). All *daf-2* phenotypes are suppressed when in combination with a reduction-of-function mutation in *daf-16*. Therefore, DAF-16 activity is critical to the observed longevity, and *daf-16;daf-2* double mutants are devoid of the long-lived phenotype (Kenyon et al., 1993). Downstream transcriptional targets of DAF-16 have been investigated using global transcriptomic and proteomic methods. Targeted transcriptomic studies have focused on genes involved in stress resistance due to the increased resistance to oxidative stress,

heat, and heavy metals (Barsyte et al., 2001) that is characteristic of *daf-2* mutants. These targeted studies identified the upregulation of transcripts for superoxide dismutase (*sod-3*), metallothionein (*mtl-1*), and heat-shock proteins (*hsp-16*) (Barsyte et al., 2001; Honda and Honda, 1999; Walker et al., 2001). Global transcriptomic analysis identified upregulated genes that encode proteins involved in metabolism, steroid and lipid synthesis, and dauer formation. Downregulated genes were involved in translation elongation, protein degradation, apolipoproteins, and peptide and lipid transport (Jensen et al., 2006; Lamitina and Strange, 2005; Murphy et al., 2003; Oh et al., 2006; Tullet, 2015; Yu et al., 2008; McElwee et al., 2003, 2004). In addition to transcriptomic profiling, global proteomic analyses of *daf-2* mutants using stable isotope labeling and quantitative mass spectrometry (MS) identified several protein-abundance changes that were not detected in the microarray analyses (Depuydt et al., 2013, 2014; Dong et al., 2007), underscoring the complementarity of different global profiling techniques such as transcriptomics and proteomics.

Due to a plethora of protein posttranslational modifications, protein-protein interactions, and endogenous inhibitors, protein abundance is not a direct measure of activity state (Walsh et al., 2005). To complement abundance-based global profiling methods such as transcriptomics and proteomics, the field of activity-based protein profiling (ABPP) has evolved to directly measure protein activity in complex proteomes (Adam et al., 2002; Evans and Cravatt, 2006). Here, we apply the tools of ABPP, specifically reactivity-based proteomics, to profile changes associated with impaired IIS in *C. elegans*.

ABPP studies typically focus on a particular enzyme class of interest, and here, we focus on cysteine-mediated protein activities by applying cysteine-reactivity profiling, which monitors changes in cysteine reactivity across two or more proteomes (Deng et al., 2013; Pace and Weerapana, 2014; Wang et al., 2014; Weerapana et al., 2010). Cysteine residues on proteins serve critical functions in catalysis and regulation (Pace and Weerapana, 2013). Diverse protein families, including proteases, kinases, and oxidoreductases, contain cysteine residues that are essential for protein function. These functional cysteines demonstrate elevated reactivity, allowing for enrichment of proteins with functional cysteines by using cysteine-reactive electrophilic probes (Weerapana et al., 2010). In *C. elegans*, proteins involved in stress resistance, such as heat-shock proteins (Hsu et al., 2003), oxidoreductases (e.g., peroxiredoxins) (Zarse et al., 2012), and detoxifying enzymes (e.g., glutathione S-transferases) (Ayyadevara et al., 2007), are regulated by the IIS pathway and rely on critical cysteine residues for function. Several of these and other cysteine-containing proteins are low in abundance and intractable to standard abundance-based proteomic analyses. Cysteine-reactivity profiling can allow for monitoring abundance changes among these IIS-relevant proteins by enriching low-abundance proteins within this class for enhanced detection.

Dysregulated reactive oxygen species (ROS) is a characteristic feature of impaired IIS (Honda and Honda, 1999; Zarse et al., 2012). ROS can target cysteine residues within proteins (Couvertier et al., 2014), resulting in changes to the oxidation state and subsequent function of diverse cysteine-containing proteins. The relationship between ROS and lifespan extension through IIS is complex and multifaceted. Acute inhibition of DAF-2 results in a transient increase in ROS levels due to an increase in metabolic rate to compensate for decreased glucose uptake; this spike in ROS then triggers the activation of a variety of antioxidant systems and the subsequent lowering of ROS levels (Zarse et al., 2012). Therefore, chronic inactivation of DAF-2 results in sustained increases in expression of antioxidant enzymes such as superoxide dismutase 3 (SOD3) and catalase, which render lower ROS levels in *daf-2* mutants (Honda and Honda, 1999). Due to the sensitivity of cysteine-mediated protein activities to changes in ROS, the abundance of these proteins is not a true representation of activity state. Cysteine-reactivity profiling can therefore serve to identify cysteine oxidation events that occur during IIS. Previous studies have applied redox-proteomic methods to identify *C. elegans* proteins that are oxidized upon exposure to peroxide (Kumsta et al., 2011), but similar studies have not been utilized to explore endogenous oxidative events associated with impaired IIS.

In summary, comparing changes in cysteine reactivity across *daf-2* and *daf-16*;*daf-2* mutants allows identification of changes in protein abundance and/or oxidation driven by impaired IIS. We applied a promiscuous cysteine-reactive chemical probe, coupled with quantitative MS (Qian et al., 2013; Weerapana et al., 2010), to globally quantify cysteine-reactivity changes between *daf-2* and *daf-16*;*daf-2* mutants. Our studies identified 40 cysteine-containing proteins that show a greater than 2-fold change in cysteine reactivity upon impaired IIS. Subsequent RNAi-mediated knockdown of 12 genes identified *lbp-3* and *K02D7.1* as novel modulators of *C. elegans* lifespan and dauer formation. Importantly, our studies represent one of the first applications of the tools of ABPP in *C. elegans* and highlight the ability of chemical proteomics to complement traditional transcriptomic and proteomic methods used to study IIS.

RESULTS

Reactive-Cysteine Profiling Reveals Functional Cysteines in *C. elegans*

Cysteine is one of the most intrinsically nucleophilic amino acids, and this nucleophilicity can be modulated by the protein microenvironment to enable diverse biochemical functions (Giles et al., 2003; Pace and Weerapana, 2013). A global proteomic evaluation of cysteine reactivity demonstrated that functional cysteines involved in catalysis and regulation display elevated reactivity relative to non-functional cysteines in the proteome (Weerapana et al., 2010). In this previous study, the intrinsic reactivity of hundreds of cysteines in human proteomes was monitored using a promiscuous cysteine-reactive iodoacetamide-alkyne (IA) probe. Comparison of the extent of cysteine labeling as a function of time or IA concentration revealed a subset of hyperreactive cysteines that saturated labeling at low time points or low IA concentrations. This subset of hyperreactive cysteines was enriched in functional cysteines (Weerapana et al., 2010). To determine whether a similar strategy would allow identification of functional cysteines in *C. elegans* lysates, we performed a concentration-dependent analysis of cysteine labeling by the IA probe.

Lysates from *daf-16*;*daf-2* mutants were used for these studies. These lysates were treated with either 10 μM or 100 μM IA probe prior to conjugation to isotopically labeled,

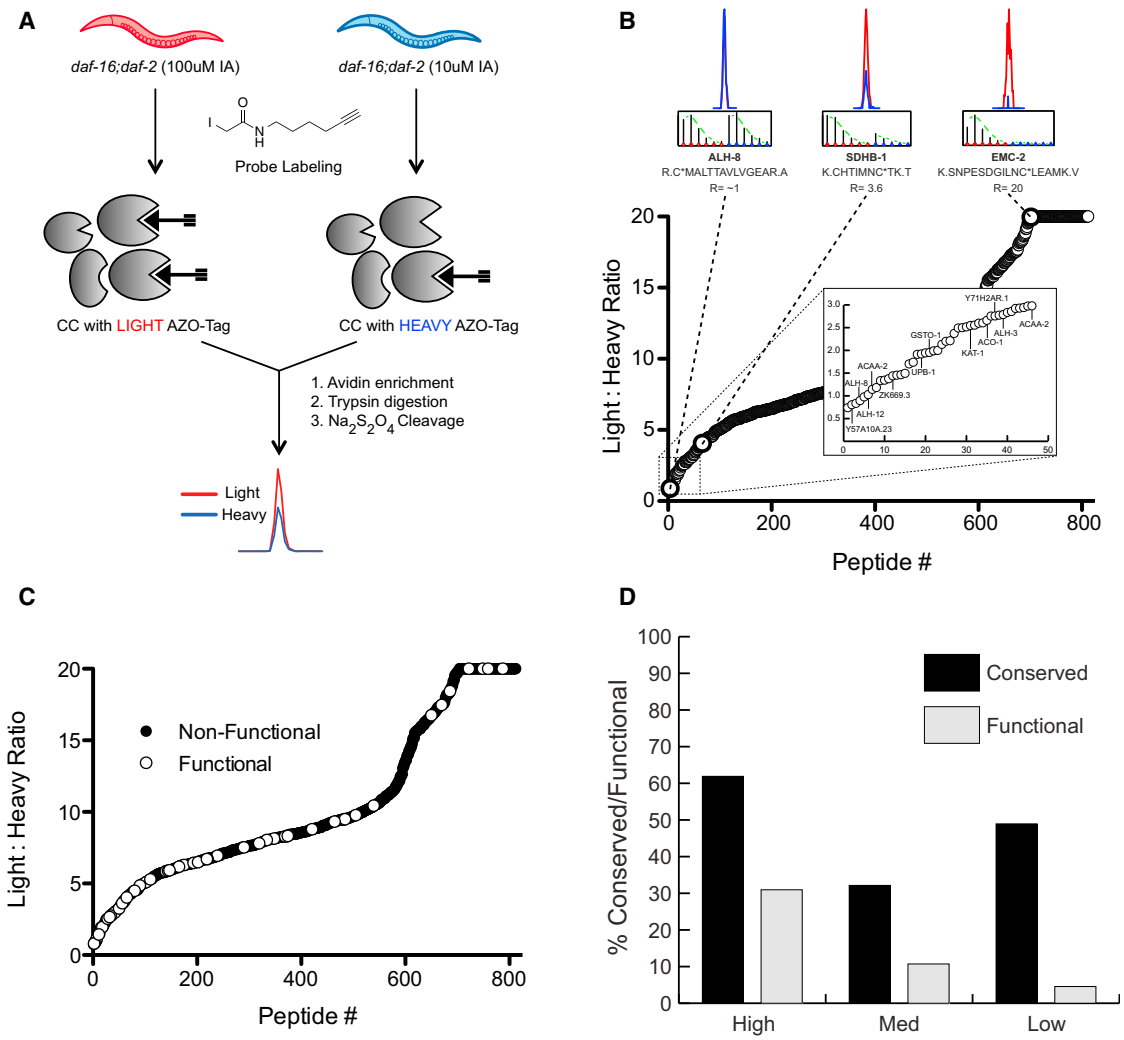

Figure 1. Identifying Hyperreactive Cysteines in *C. elegans* Lysates

(A) Workflow to identify hyperreactive cysteines in the *daf-16*;*daf-2* mutant proteome. *C. elegans* lysates were treated with either 10 μM or 100 μM IA probe and conjugated to the heavy (10 μM IA) or light (100 μM IA) Azo tags via click chemistry (CuAAC). The samples were combined and then enriched with streptavidin beads, and subjected to on-bead trypsin digestion and $Na_2S_2O_4$ treatment to release the probe-labeled peptides from the beads for quantitative LC/LC-MS/MS analysis.

(B) Cysteine-containing peptides (N = 816) in order from high (light/heavy ratio <3) to low (light/heavy ratio >>3) reactivity. Singleton peptides that are only detected in the Azo-L sample are designated an arbitrary R value of 20. Chromatograms and isotopic envelopes of representative peptides are shown above the plot with high (ALH-8, R = 1.0), medium (SDHB-1, R = 3.6), and low (EMC-2, R = 20) cysteine reactivity. Chromatograms and isotopic envelopes for the light peptides are in red and the heavy peptides are in blue. Inset displays 46 peptides with the lowest light/heavy ratio values representing the most reactive cysteines in the *daf-16*;*daf-2* mutant proteome. Proteins containing cysteines with annotated biological function shown in Table 1 are labeled.

(C) Cysteines with an annotated biological function in either *C. elegans* or the corresponding human homolog are highlighted in white along the ratio plot.

(D) Cysteine-containing peptides were sorted into three groups of light/heavy ratios: R < 3 (hyperreactive), R = 3–6 (medium reactivity), and R > 6 (low reactivity). The percentages of cysteines in each grouping that are conserved in humans (black) or have annotated biological function (gray) are shown.

chemically cleavable biotin tags (Azo tags) (Qian et al., 2013) using copper(I)-catalyzed azide-alkyne cycloaddition (CuAAC) (Rostovtsev et al., 2002). The Azo tags comprise an azide for CuAAC-mediated conjugation to IA-labeled proteins, a biotin for enrichment of labeled proteins on streptavidin beads, a chemically cleavable azobenzene linker for selective release of probe-labeled peptides, and an isotopically light or heavy valine residue for quantitation of labeled peptides in two different proteomes. *C. elegans* lysates treated with 10 μM and 100 μM IA were conjugated to heavy and light Azo tags, respectively. These samples were then combined and subjected to streptavidin enrichment, on-bead trypsin digestion, and treatment with sodium dithionite to release the probe-labeled peptides for analysis by high-resolution tandem liquid chromatography (LC/LC)-tandem MS (MS/MS) (Figure 1A). MS analysis identified 816 unique cysteine-containing peptides in the *daf-16*;*daf-2* lysates with calculated light/heavy ratio (R) values in at least two out of four replicates (Table S1). The R values reflect the degree of cysteine labeling between the 10- and 100-μM IA-treated samples. A cysteine that is hyperreactive and saturates labeling at

Table 1. Functional Cysteines Identified in *C. elegans*

Gene Symbol	Protein Name	Sequence	Ratio	Function
Y57A10A.23	thioredoxin domain-containing protein 12[a]	K.SWC*HACK.A	0.805	redox-active disulfide
alh-8	methylmalonate semialdehyde dehydrogenase	R.C*MALTTAVLVGEAR.A	0.898	active-site nucleophile
alh-12	aldehyde dehydrogenase[a]	–AMLANFLNQGQVC*TNATR.V	1.03	active-site nucleophile
acaa-2	acetyl-CoA acyltransferase 2	R.LC*GSGFQAVVNAAQAIK.L	1.15	acyl-thioester intermediate
ZK669.3	γ-interferon-inducible lysosomal thiol reductase[a]	R.C*SDTSYWMK.W	1.44	redox-active disulfide
upb-1	ureidopropionase β[a]	R.IGINIC*YGR.H	1.92	active-site nucleophile
gsto-1	glutathione transferase ω-1	R.FC*PWAER.A	1.96	active-site nucleophile
kat-1	acetyl-CoA acetyltransferase	K.VC*SSGLK.A	2.55	acyl-thioester intermediate
aco-1	aconitate hydratase	K.IGFNIAGYGC*MTCIGNSGP-	2.66	iron binding
Y71H2AR.1	thioredoxin domain-containing protein 17[a]	K.ILTTGESWC*PDCVVAEPVV-	2.76	active-site nucleophile/ redox-active disulfide
alh-3	formyltetrahydrofolate dehydrogenase	K.GENC*IAAGR.V	2.79	active site
acaa-2	acetyl-CoA acyltransferase 2	K.YGIGSAC*IGGGQGIAILFEK-	2.98	active site

Hyperreactive cysteines identified in the *daf-16*;*daf-2* mutant proteomes with an annotated biological function in either *C. elegans* or human UniProt databases.
[a]Human homolog of unannotated *C. elegans* proteins.

the low IA concentration will display R values of ~1, whereas less reactive cysteines will display R values of >>1. The 816 cysteine-containing peptides that were identified displayed a wide range of R values (Figures 1B and S1), with 46 cysteines demonstrating R values <3 (Figure 1B, inset).

To determine whether those cysteines with low ratio values (R < 3) were enriched in known functional residues, we mined the *C. elegans* UniProt database for functional annotation of the identified cysteines as catalytic or regulatory residues. However, the *C. elegans* UniProt entries have poor annotation of residue and protein functions. Therefore, a BLAST search was performed for each identified *C. elegans* protein against the human UniProt database, identifying cysteine residues that were conserved in the corresponding human homolog and were functionally annotated to be involved in catalysis and regulation (Table S1). Comparing functional annotation with the observed R values for each cysteine demonstrated that cysteines with low R values (i.e., hyperreactive cysteines) were enriched in known functional residues (Figure 1C), similar to what was observed in human proteomes (Weerapana et al., 2010). Approximately 30% of all cysteines identified with ratios <3 are known to be functional in either *C. elegans* or the corresponding human homolog (Figure 1D), in contrast to <5% of cysteines with R > 6 that were annotated to be functional. A similar trend in cysteine conservation was also observed (Figure 1D), albeit with lower enrichment among the hyperreactive subset of cysteines, suggesting that cysteine reactivity, rather than conservation, is a more effective predictor of cysteine functionality. Functionally annotated hyperreactive cysteines in *C. elegans* include active-site cysteines in glutathione S-transferases, aldehyde dehydrogenase, and acetyl-coenzyme A (CoA) acyltransferases (Table 1). These studies constitute the first evaluation of cysteine reactivity in *C. elegans* and provide a list of annotated and unannotated hyperreactive cysteines for future functional characterization.

Chemical-Proteomic Analysis Identifies Changes in Cysteine Reactivity between *daf-2* and *daf-16*;*daf-2* Mutants

Given that the IA probe labels a large number of functionally relevant cysteine residues in *C. elegans*, cysteine reactivity was compared across *daf-2* and *daf-16*;*daf-2* mutants. These studies reveal variations in protein abundance and cysteine posttranslational-modification state in the long-lived *daf-2* mutants relative to the *daf-16*;*daf-2* mutants. Initially, to confirm the longevity phenotype of the *daf-2* mutants, we performed a lifespan assay on WT (N2), *daf-2*, and *daf-16*;*daf-2* mutants cultured under identical conditions. As expected, *daf-2* mutants demonstrated an almost 100% lifespan extension (Figure S2A) (Kenyon et al., 1993). To quantify cysteine-reactivity changes between *daf-2* and *daf-16*;*daf-2* mutants, we treated lysates from *daf-2* and *daf-16*;*daf-2* animals with 100 μM IA, appended to Azo-L and Azo-H, respectively, and subjected them to the MS workflow utilized previously (Figure 2A). The higher concentration of IA (100 μM) was utilized for these comparative studies to maximize the number of cysteine residues identified, and is consistent with previous cysteine-reactivity profiling experiments in lysates treated with oxidants (Deng et al., 2013), Zn^{2+} ions (Pace and Weerapana, 2014), and lipid-derived electrophiles (Wang et al., 2014). MS analysis provided R values for 338 cysteine-containing peptides on 254 proteins (Figures 2B and S2B; Table S2) from two biological replicates.

High R values are indicative of cysteines with increased reactivity in *daf-2* mutants, whereas low R values represent cysteines with decreased reactivity in *daf-2* mutants. The majority of identified cysteines (84.9%) demonstrated R values in the range 0.5 < R < 2, demonstrating less than 2-fold change across the *daf-2* and *daf-16*;*daf-2* proteomes (Table S2). In total, 50 cysteine residues on 40 proteins displayed a ≥2-fold change (Tables 2 and 3), with 36 showing increases and 14 showing decreases in *daf-2* mutants. These top 40 proteins were compared

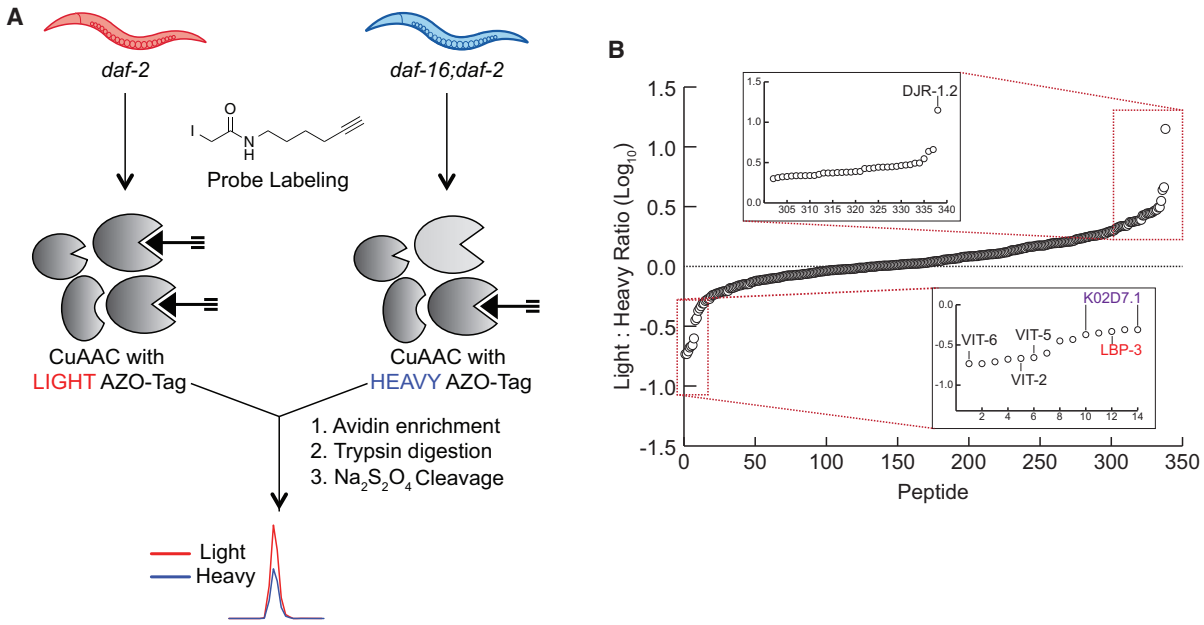

Figure 2. Identifying Cysteine-Reactivity Changes between *daf-2* and *daf-16;daf-2* Mutants

(A) Workflow to quantify cysteine-reactivity changes between *daf-2* and *daf-16;daf-2* mutants. Lysates from each mutant were treated with 100 μM IA probe, conjugated to either the light (*daf-2*) or heavy (*daf-16;daf-2*) Azo tags, and subjected to streptavidin enrichment, tryptic digest, and $Na_2S_2O_4$ cleavage as before. (B) Cysteine-containing peptides (N = 338) were identified and the $\log_{10}$ value of each light/heavy ratio was plotted; $\log_{10}$ values less than 0 indicate cysteines that have decreased reactivity in *daf-2* mutants, whereas $\log_{10}$ values greater than 0 indicate cysteines with increased reactivity in *daf-2* mutants. Insets display peptides with cysteines that show at least a 2-fold increase (upper) or decrease (lower) in reactivity in *daf-2* mutants. Proteins with a previously observed role in lifespan regulation (DJR-1.2, Vit-2, -5, -6) and those that we demonstrate to affect lifespan upon RNAi-mediated knockdown (LBP-3, K02D7.1) are specifically indicated.

with transcriptomic data available for *daf-2* and *daf-16;daf-2* mutants (McElwee et al., 2003, 2004), to determine whether the changes we observed were also present at the transcript level. Transcriptomic data was available for 25 of the 40 proteins and in terms of the general trend (increase versus decrease in *daf-2* animals), all but one hit (protein Y39E4A.3) agreed with the previously reported transcriptomic data (Tables 2 and 3). Further comparison of these 40 proteins to proteomic studies that measured protein-abundance changes in *daf-2* mutants (Depuydt et al., 2013) demonstrated poor overlap between the proteins identified in unenriched proteomics compared with cysteine enrichment. Specifically, only 19 of the 40 (48%) were identified in these previous global proteomic studies (Depuydt et al., 2013) (Tables 2 and 3). This poor overlap underscores the ability of cysteine enrichment to promote the identification of low-abundance proteins that are typically suppressed in unenriched proteomic analyses. Of the 19 proteins identified in both cysteine enrichment and unenriched proteomic analyses, 13 showed the same changes (increase versus decrease in *daf-2* animals), while the remaining six (PES-9, RPS-12, RPS-17, DHS-25, HEL1, and INF-1) showed changes that were not statistically significant in the unenriched proteomic studies (Depuydt et al., 2013). Lastly, the cysteines identified in our study were also compared with a redox-proteomic study in WT *C. elegans* that utilized the OxiCAT method to identify sites of cysteine oxidation upon hydrogen peroxide exposure (Kumsta et al., 2011). Only 13 of the 338 cysteine residues from our study were identified in the OxiCAT data (Table S3), and only one of these cysteine residues (on RPS-17) were within the 40 proteins that demonstrated a ≥2-fold change between *daf-2* and *daf-16;daf-2* mutants.

Several of the protein targets we identified have been previously characterized using RNAi knockdown and phenotypic analysis, including the vitellogenins (VIT-2, -5, and -6) and the DJR-1.2 glyoxalase (Fischer et al., 2013; Lee et al., 2013; Murphy et al., 2003; Yuan et al., 2012). The vitellogenins showed the largest decrease in *daf-2* mutants, and DJR-1.2 showed the largest increase in *daf-2* mutants according to our cysteine-profiling data (Tables 2 and 3). Vitellogenesis is the process of egg yolk, or vitellogenin, production that provides the major nutrient source for developing embryos. Vitellogenesis is suppressed in the *daf-2* mutant, possibly extending lifespan by using those resources to maintain somatic cells (DePina et al., 2011). Vitellogenins are among the most downregulated proteins in *daf-2* mutants according to previous transcriptomic and proteomic analyses (Depuydt et al., 2013; Dong et al., 2007; McElwee et al., 2003; McElwee et al., 2004), and RNAi-mediated knockdown lengthened the lifespan of *daf-2*(+) animals (Murphy et al., 2003). DJR-1.2 is homologous to the human DJ-1 protein, and defects in the *dj-1* gene are a cause of autosomal recessive early-onset Parkinson's disease (Bonifati et al., 2003). DJ-1 is a multifunctional redox-sensitive protein that plays roles in dampening mitochondrial oxidative stress and regulation of anti-apoptotic and antioxidant gene expression. DJ-1 also regulates Toll-like receptor signaling, suggesting a role in innate immunity (Cornejo Castro et al., 2010). *djr-1.2* has been found to be upregulated in both *daf-2* and dauer larva, and shows a

Table 2. Cysteine Residues Identified with Decreased Reactivity ≥2-Fold in *daf-2* Relative to *daf-16;daf-2* Mutants

Gene ID	Symbol	Description	Sequence	Average Ratio	Transcriptomic Data	Proteomic Data
K07H8.6	vit-6	vitellogenin-6	VIC*PIAEVGTK	0.185 ± 0.005	decreased	decreased
			TEEGLIC*R	0.185 ± 0.025		
			EC*NEEQLEQIYR	0.195 ± 0.005		
			SYANNESPC*EQTFSSR	0.21 ± 0.01		
			NQFTPC*YSVLAK	0.25 ± 0.02		
C42D8.2	vit-2	protein VIT-2, isoform b	VAIVC*SK	0.215 ± 0.005	decreased	not identified
C04F6.1	vit-5	vitellogenin-5	APLTTC*YSLVAK	0.22 ± 0.01	decreased	decreased
ZK228.3	ZK228.3	protein ZK228.3	DGVVYSVAC*STHQFV	0.355 ± 0.015	decreased	not identified
C17H12.13	C17H12.13	protein C17H12.13, isoform b	DLVQDSLQC*SSTCVIR	0.37 ± 0.01		not identified
K02D7.1	K02D7.1	protein K02D7.1	ADLGIIC*GSGLGPIGDTVQDATILPYSK	0.425 ± 0.025		not identified
			TVGADALGMSTC*HEVTVAR	0.49 ± 0.05		
R11H6.1	pes-9	protein PES-9	EGC*SIPITLTFQELTGK	0.445 ± 0.035	decreased	no change
F40F4.4	lbp-3	fatty acid-binding protein homolog 3	MVNNGITC*R	0.465 ± 0.015	decreased	not identified
F32D1.5	F32D1.5	probable GMP reductase	SAC*TYTGAK	0.49 ± 0.02		decreased

The 14 cysteines on nine proteins that demonstrated decreased reactivity in *daf-2* ($R \leq 0.5$) are shown. Transcriptomic changes (decreased or increased in *daf-2*) of the corresponding genes previously identified in microarray analysis of *daf-2* and *daf-16;daf-2* are shown (McElwee et al., 2003; McElwee et al., 2004). Proteomic changes for these proteins in unenriched proteomic analyses (decreased, increased, or no change in *daf-2*) are also indicated (Depuydt et al., 2013). "Not identified" indicates a protein that was not present in the unenriched proteomic datasets.

DAF-16-dependent decrease in stress resistance and viability upon knockdown (Lee et al., 2013). These well-characterized lifespan-modulating effects for vitellogenins and DJR-1.2, the two most significantly changed proteins from our data, serves as validation of our platform to identify potential mediators of IIS and lifespan.

RNAi-Mediated Knockdown of *lbp-3* and *K02D7.1* Results in Modulation of Lifespan and Dauer Formation

To determine whether other proteins identified in our cysteine-reactivity profiling studies were implicated in IIS-mediated lifespan regulation, we performed RNAi-mediated knockdown studies followed by lifespan analyses. For these RNAi studies, we focused on a set of 20 genes, corresponding to the ten proteins that showed the largest decrease (*vit-6*, *vit-2*, *vit-5*, *ZK228.3*, *C17H12.13*, *K02D7.1*, *pes-9*, *lbp-3*, *F32D1.5*, and *eef-2*) and the ten proteins with the largest increase (*djr-1.2*, *F20G2.2*, *sodh-1*, *pck-1*, *moc-2*, *rab-14*, *ZK829.7*, *gspd-1*, *inf-1*, and *F20D6.11*) in *daf-2* mutants, consistent across the two biological replicates from our cysteine-profiling data (Table S2). Of these 20 genes, in addition to the vitellogenin (*vit-6/-2/-5*) and *djr-1.2* genes discussed previously, four other genes had already been subjected to RNAi and phenotypic analysis (*sodh-1* [Murphy et al., 2003]; *eef-2* [Li et al., 2011]; *inf-1* [Curran and Ruvkun, 2007]; and *pck-1* [Yuan et al., 2012]). The remaining 12 genes with no previous RNAi and phenotypic data related to lifespan were targeted for RNAi-mediated knockdown using bacterial strains from the Ahringer RNAi library (Kamath et al., 2003), and lifespan assays were performed with respect to vector-treated controls (Table S4 and Figure S3). We observed a greater than 15% increase in lifespan for four of the genes tested (*K02D7.1*, *pes-9*, *lbp-3*, and *gspd-1*).

To determine whether inactivation of these four genes would further augment dauer formation in *daf-2* mutants, we performed dauer-arrest assays upon RNAi-mediated knockdown. Reduction of levels of both LBP-3 and K02D7.1 increased dauer formation by 23% and 37%, respectively (Figure 3C and Table S4). In contrast, knockdown of *pes-9* and *gspd-1* showed a decrease in dauer formation (Table S4). Therefore, these data implicate *C. elegans* LBP-3 and K02D7.1 proteins in both lifespan regulation (Figures 3A and 3B; Table S5) and entry into the dauer state (Figure 3C and Table S4). RT-PCR was used to confirm knockdown of *lbp-3* and *K02D7.1*, and compared against the control gene *pmp-3*, which demonstrates unusually stable expression levels with little variation between adults, dauers, and L3 larvae, or between WT and *daf-2* or *daf-16* mutant adults (Figure 3D) (Hoogewijs et al., 2008). To determine whether the observed effects on lifespan were dependent on the presence of functional DAF-2 and DAF-16, we repeated lifespan assays in the background of *daf-16* mutants, *daf-16;daf-2* double mutants, and WT (N2) animals (Figure S4). Knockdown of *lbp-3* only affected the lifespan of *daf-2* mutants, whereas *K02D7.1* knockdown extended the lifespan in all mutant backgrounds.

DISCUSSION

Global profiling techniques, such as transcriptomics and proteomics, can provide valuable insight into changes in mRNA and protein across multiple biological samples. These studies are

Table 3. Cysteine Residues Identified with Increased Reactivity ≥2-Fold in *daf-2* Relative to *daf-16*;*daf-2* Mutants

Gene ID	Symbol	Description	Sequence	Average Ratio	Transcriptomic Data	Proteomic Data
F54E7.2	rps-12	40S ribosomal protein S12	GLHETC*K	2 ± 0.12		no change
Y39E4A.3	Y39E4A.3	protein Y39E4A.3, isoform a	GYTMENFMNQC*YGNADDLGK	2.06 ± 0.2	decreased	not identified
C08B11.7	ubh-4	probable ubiquitin C-terminal hydrolase ubh	GHC*LSNSEEIR	2.105 ± 0.135		not identified
R03D7.6	gst-5	probable glutathione S-transferase 5	ETC*AAPFGQLPFLEVDGK	2.125 ± 0.025		not identified
F36H1.6	alh-3	protein ALH-3	GENC*IAAGR	2.155 ± 0.115		not identified
Y54E10BR.6	rpb-7	protein RPB-7	LFNEVEGTC*TGK	2.175 ± 0.335		not identified
T20G5.1	chc-1	probable clathrin heavy chain 1	AAIGQLC*EK	2.175 ± 0.825		increased
K08E3.5	K08E3.5	protein K08E3.5, isoform f	LNGGLGTSMGC*K	2.18 ± 0.04		not identified
T08B2.10	rps-17	40S ribosomal protein S17	VC*DEVAIIGSK	2.185 ± 0.105		no change
F09E10.3	dhs-25	protein DHS-25	TPMTEAMPPTVLAEIC*K	2.19 ± 0.02		no change
K11H3.1	gpdh-2	protein GPDH-2, isoform c	NVVAC*AAGFTDGLGYGDNTK	2.26 ± 0.06		not identified
K12G11.3	sodh-1	alcohol dehydrogenase 1	LMNFNC*LNCEFCK	2.35 ± 0.21	increased	increased
			LMNFNCLNC*EFCK	2.35 ± 0.21		
			LMNFNCLNCEFC*K	2.35 ± 0.21		
			DTNLAAAAPILC*AGVTVYK	4.355 ± 0.135		
C26D10.2	hel-1	spliceosome RNA helicase DDX39B homolog	YFVLDEC*DK	2.38 ± 0.05		no change
W05G11.6	pck-2	protein W05G11.6, isoform a	AELMNPAGIYIC*DGSQK	2.385 ± 0.065	increased	increased
			TNAMAMESC*R	2.405 ± 0.155		
			FIAAAFPSAC*GK	3.53 ± 0.13		
C36A4.9	acs-19	protein ACS-19, isoform a	TNISYNC*LER	2.41 ± 0.14	increased	not identified
F55H12.4	F55H12.4	protein F55H12.4	GSTGHC*YK	2.45 ± 0.18	increased	increased
Y113G7B.23	swsn-1	protein SWSN-1	GVQAAAASC*LAAAAVK	2.455 ± 0.245		not identified
ZK829.4	gdh-1	glutamate dehydrogenase	CDIFVPAAC*EK	2.67 ± 0.37		not identified
C05C10.6	ufd-3	protein UFD-3, isoform b	ALAVTQGGC*LISGGR	2.71 ± 0.04		not identified
K08F4.9	dhs-12	protein DHS-12	AAIVNIGSDC*ASQALNLR	2.77 ± 0.17	increased	increased
F01G10.1	tkt-1	protein TKT-1	ISSIEMTC*ASK	2.775 ± 0.225	increased	increased
B0286.3	B0286.3	probable multifunctional protein ADE2	MPNGIGC*TTVLDPSEAALAAAK	2.785 ± 0.095	increased	increased
F32A7.5	F32A7.5	protein F32A7.5, isoform d	DISGEQLQAILC*GK	2.805 ± 0.015		not identified
F20D6.11	F20D6.11	protein F20D6.11	FSGC*NQGSTK	2.84 ± 0.48	increased	not identified
F57B9.6	inf-1	eukaryotic initiation factor 4A	AIVPC*TTGK	2.905 ± 0.155		no change
B0035.5	gspd-1	glucose-6-phosphate 1-dehydrogenase	SSC*ELSTHLAK	2.95 ± 0.36		increased
ZK829.7	ZK829.7	protein ZK829.7	AILEVC*DPSSALDADQSGGVPIPAATSE	2.98 ± 0.31	increased	increased
K09A9.2	rab-14	protein RAB-14	AFAEENGLTFLEC*SAK	3.11 ± 1.7		not identified
W01A11.6	moc-2	protein MOC-2	VCVITVSDTC*SAGTR	3.125 ± 0.125		not identified
F20G2.2	F20G2.2	protein F20G2.2	SC*SIDLAK	4.59 ± 0.55		increased
C49G7.11	djr-1.2	protein DJR-1.2	LAEC*PVIGELLK	14.115 ± 1.505	increased	not identified

The 36 cysteines on 31 proteins that demonstrated increased reactivity in *daf-2* (R ≥ 2) are shown. Transcriptomic changes (decreased or increased in *daf-2*) of the corresponding genes previously identified in microarray analysis of *daf-2* and *daf-16*;*daf-2* are shown (McElwee et al., 2003, 2004). Proteomic changes for these proteins in unenriched proteomic analyses (decreased, increased, or no change in *daf-2*) are also indicated (Depuydt et al., 2013). "Not identified" indicates a protein that was not present in the unenriched proteomic datasets.

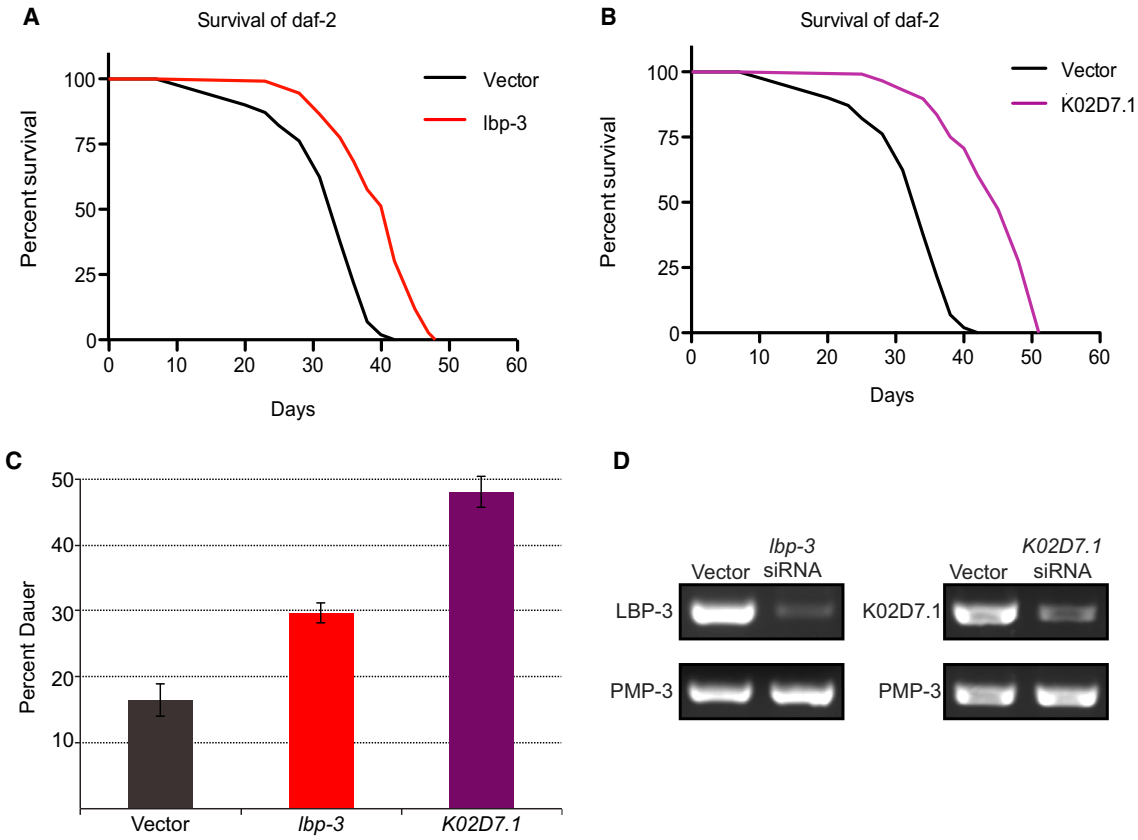

Figure 3. RNAi-Mediated Knockdown and Phenotypic Analysis

(A and B) Survival plots of *daf-2* mutants treated with (A) *lbp-3* small interfering RNA (siRNA) or (B) *K02D7.1* siRNA and compared with a vector-treated control.

(C) Dauer-arrest assay comparing the percent dauer formation of *daf-2* mutants with RNAi-mediated knockdown of *lbp-3* and *K02D7.1* compared with a vector-treated control. Error bars reflect SD from three replicates.

(D) RT-PCR of *daf-2* mutants treated with *lbp-3* or *K02D7.1* siRNA using primers for *lbp-3*, *K02D7.1*, or *pmp-3* as a control.

complemented by chemical-proteomic methods that apply chemical probes to enrich specific subsets of the proteome. Chemical-proteomic platforms, such as ABPP, can enrich low-abundance proteins that are intractable to whole-proteome analyses, and can additionally provide insight into posttranslational modifications that can activate or inactive proteins. Despite the application of ABPP to identify dysregulated protein activities in a variety of human, mouse, and bacterial proteomes, these tools are yet to be applied in *C. elegans*. Here, we apply cysteine-reactivity profiling to uncover hyperreactive and functional cysteines in *C. elegans* and identify proteins dysregulated during impaired IIS. We identified a subset of hyperreactive cysteines in *C. elegans* and demonstrate that ~30% of these cysteines are known to perform essential roles in catalysis and regulation in the corresponding human homologs. Further studies into the unannotated hyperreactive cysteines that we identified are likely to reveal novel functional cysteine residues and serve to further annotate the *C. elegans* proteome.

Comparing cysteine reactivity in *daf-2* and *daf-16*;*daf-2* proteomes revealed 40 proteins that displayed a >2-fold change. The majority of these changes have been previously reported in transcriptomic studies, serving to verify the accuracy of our platform to identify changes across *daf-2* and *daf-16*:*daf-2* proteomes. Importantly, several of these proteins, such as the vitellogenins and DJR-1.2, have also been functionally characterized to be important mediators of IIS and lifespan, further alluding to the promise of global profiling studies to reveal functional components of the IIS pathway. Importantly, many of the proteins identified were not detected in previous unenriched proteomic studies, highlighting the promise of ABPP and cysteine reactivity-profiling studies to enrich for low-abundance proteins inaccessible to unenriched proteomics. To investigate previously uncharacterized proteins that were identified in our studies, we performed RNAi-mediated knockdown and subsequent phenotypic assays to monitor lifespan and dauer formation. These studies revealed that RNAi-mediated knockdown of *lbp-3* and *K02D7.1* results in significant increases in both lifespan and dauer formation, implicating these proteins as important components of the IIS pathway.

LBP-3 is an intracellular lipid chaperone in the fatty acid-binding protein (FABP) family. FABPs are conserved from *C. elegans* to humans and are involved in fatty acid uptake, transport, and oxidation (Storch and Corsico, 2008). The *C. elegans* genome contains nine LBP genes and the exact functions of these individual LBPs remains unclear (Plenefisch et al., 2000). Of the *C. elegans* LBPs, LBP-5 appears to be the most extensively

studied, whereby RNAi-mediated knockdown of *lbp-5* results in fat accumulation in the intestine (Xu et al., 2011). The putative role of the *C. elegans* LBPs in fat accumulation is notable because a characteristic feature of the *daf-2* mutants and long-lived dauers is increased fat content (Kimura et al., 1997). Previous studies have also shown that mutational inactivation of other lipid transport proteins, such as the intramembrane transporters, NDG-4 and NRF-5/6, increase stress resistance and lifespan through the IIS pathway (Brejning et al., 2014). These previous studies of the LBP family and related proteins support a potential role for LBP-3 in *C. elegans* lipid metabolism and IIS.

Given the lack of functional characterization of the *C. elegans* LBPs, we probed the mammalian FABPs for insight into the function and regulation of this class of proteins. There are at least nine human FABPs and these have distinct tissue localization patterns. All FABPs are small intracellular proteins that can localize to the nucleus (Furuhashi and Hotamisligil, 2008; Smathers and Petersen, 2011) and bind long-chain fatty acids, albeit with different binding affinities. In our cysteine-profiling studies, we identified Cys154 as labeled by the IA probe; this cysteine is not annotated as functional in the *C. elegans* UniProt database, but is conserved in several of the human FABPs (Figure S5A). *C. elegans* LBP-3 shares the most homology with human FABP-5 (27% sequence identity), which contains a disulfide bond between Cys120 and Cys127 that regulates protein structure and function under reducing/oxidizing conditions (Hohoff et al., 1999). In fact, several FABPs have been shown to be oxidized, glutathionylated, and/or modified by oxidized lipid species such as 4-hydroxynonenal at cysteine, with effects on the lipid-binding ability and proteolytic stability (Bennaars-Eiden et al., 2002; Smathers et al., 2012, 2013; Yang et al., 2014). It is therefore likely that Cys154 in *C. elegans* LBP-3 is similarly regulated through redox modifications. Interestingly, the 2.2-fold decrease in IA-labeled LBP-3 that we observed in the *daf-2* animals is significantly less than the change reported for *lbp-3* using transcriptomic analyses (~5-fold decrease). This suggests that either there is poor correlation between *lbp-3* mRNA and protein levels, or there is reduced enrichment due to partial oxidation of Cys154 *in daf-16*;*daf-2* mutants. The higher levels of ROS observed in *daf-16*;*daf-2* double mutants supports the possibility of increased protein oxidation in this strain compared with the single *daf-2* mutants (Honda and Honda, 1999; Zarse et al., 2012).

K02D7.1 is an uncharacterized protein in *C. elegans* but is homologous to human purine nucleoside phosphorylase (PNP), with 47% sequence identity. The IA-modified cysteines have no known functional annotation, but one of these cysteines is located in a highly conserved region (IIC*GSGLG), with conservation seen throughout humans, mice, flies, and yeast (Figure S5B). PNP catalyzes cleavage of the glycosidic bond of (deoxy)ribonucleosides, forming the corresponding free purine base and pentose-1-phosphate in the purine salvage pathway (Bzowska et al., 2000). Although PNP has not been directly implicated in IIS and lifespan regulation, the purine nucleotide synthesis pathway has been shown to be regulated by PI3K/AKT signaling, suggesting that enzymes within this pathway are under IIS control (Wang et al., 2009). Furthermore, a downstream enzyme involved in purine metabolism, xanthine dehydrogenase (XDH), was identified in a systematic screen for longevity genes in *C. elegans*. RNAi knockdown of XDH in *C. elegans* caused a ~12% increase in median lifespan (Hamilton et al., 2005), suggesting that perturbations in purine metabolism can modulate longevity. These previous studies indicate that *K02D7.1*, similar to XDH, is a regulator of *C. elegans* lifespan and is a promising target for further characterization to determine the exact biochemical function and role of this protein in IIS.

SIGNIFICANCE

Collectively, these studies constitute the first reported application of cysteine-reactivity profiling in *C. elegans*. Specifically, a cysteine-reactive chemical probe was applied to identify hyperreactive cysteines in *C. elegans*, revealing that these hyperreactive cysteines are enriched in functional residues critical to catalysis and regulation. Among the subset of hyperreactive cysteines were several unannotated cysteines for future functional characterization in *C. elegans* and other organisms in which these cysteines are conserved. Given the wide utility of *C. elegans* as a model organism for aging, and the well-characterized role of impaired IIS in regulating longevity in this organism, we applied chemical proteomics to identify dysregulated protein activities with potential implications in IIS-mediated longevity regulation. Importantly, chemical-proteomic approaches such as cysteine profiling have the advantage of identifying changes in posttranslational modifications as well as low-abundance proteins, which are intractable to abundance-based transcriptomic and proteomic approaches. Comparison of cysteine reactivity across *daf-2* and *daf-16*;*daf-2* mutants identified 40 proteins with >2-fold change across these proteomes. The majority of these changes were previously identified in transcriptomic studies and validated to regulate lifespan, serving to substantiate our chemical-proteomic data. Previously uncharacterized proteins were also identified, underscoring the complementarity of chemical-proteomic techniques to existing global transcriptomic and proteomic studies. Coupling chemical-proteomic tools with RNAi-mediated knockdown and phenotypic assays resulted in the identification of two proteins, LBP-3 and K02D7.1, as novel mediators of *C. elegans* lifespan and dauer formation.

EXPERIMENTAL PROCEDURES

C. elegans Culture and Maintenance

Worm strains were grown on OP50 *Escherichia coli*-seeded nematode growth medium (NGM) stock plates using standard *C. elegans* culturing techniques (Girard et al., 2007). All experiments used the following alleles: *daf-16* (mgDf50); *daf-2* (e1370). *C. elegans* strains were provided by the *Caenorhabditis* Genetics Center, and details on the specific *C. elegans* strains are provided in Supplemental Experimental Procedures.

Preparation of 4-Day *daf-2* and *daf-16*;*daf-2* Worm Lysates for MS Analysis

Synchronized worm populations for MS analysis were obtained by shaking ~3,000 gravid adult worms in a solution of sterile water (5.0 mL), KOH (1.0 mL, 5 M), and bleach (4.0 mL) for 5 min until only the eggs remained. The eggs were pelleted, washed with S Medium (5 × 10 mL), resuspended in S Medium (8 mL), and allowed to hatch overnight in a 15°C incubator.

The hatched L1 worms (~100,000) were aliquoted onto ten NGM plates for synchronized growth with the addition of OP50 *E. coli* (100 μL, 100 mg/mL) at 15°C. At the L4 larval stage, the worms were transferred to 25 floxuridine (FUDR)-containing plates (0.05 mg/mL) to prevent reproduction and transferred to a 25°C incubator. After 4 days of growth, worms were harvested and sonicated to provide lysates for MS analysis. Detailed protocols for growth, synchronization, FUDR treatment, harvesting, and lysis are provided in Supplemental Experimental Procedures.

Quantitative MS Analysis

For cysteine-reactivity studies, *daf-16*;*daf-2 C. elegans* lysates (2 × 500 μL, 2 mg/mL) in PBS were treated with either 10 μM or 100 μM IA for 1 hr at room temperature. For *daf-2* and *daf-16*;*daf-2* comparative studies, both lysates were treated with 100 μM IA for 1 hr at room temperature. The IA-labeled samples were conjugated to either the heavy or light azobenzene tags (100 μM) (Qian et al., 2013) using CuAAC by addition of tris(2-carboxyethyl)phosphine (1.0 mM from fresh 50× stock in water), tris(benzyltriazolylmethyl)amine ligand (100 μM from 17× stock in DMSO/t-butanol 1:4), and $CuSO_4$ (1.0 mM from 50× stock in water), and allowed to react at room temperature for 1 hr. For reactivity studies, 10 μM IA-treated samples were conjugated to the heavy tag, and 100 μM IA-treated samples were conjugated to the light tag. For *daf-2* and *daf-16*;*daf-2* comparative studies, *daf-2* lysates were conjugated to the light tag, and *daf-16*;*daf-2* lysates were conjugated to the heavy tag. After click chemistry, the IA-labeled proteins were enriched on streptavidin beads and subjected to on-bead trypsin digestion and sodium dithionite treatment, and LC-MS/MS analysis was performed on an LTQ-Orbitrap Discovery mass spectrometer (Thermo Fisher) as detailed in the Supplemental Experimental Procedures. The generated MS/MS data were searched using the SEQUEST algorithm against the UniProt *C. elegans* database. A static modification of +57.02146 on cysteine was specified to account for alkylation by iodoacetamide, and differential modifications of +456.2849 (Azo-L tag) and +462.2982 (Azo-H tag) were specified on cysteine to account for probe modifications. SEQUEST output files were filtered using DTASelect2.0.5, and quantification of light/heavy ratios was performed using the CIMAGE quantification package as previously described (Weerapana et al., 2010).

RNAi-Mediated Knockdown

RNAi bacterial clones were obtained from the Ahringer Lab RNAi feeding library (Timmons et al., 2001), and feeding plates were prepared as described in Supplemental Experimental Procedures.

Lifespan and Dauer Assays

Lifespan assays were performed using L4 animals at 20°C (30 animals per plate × 4), and scored every 2–3 days. Dauer assays were performed at 22.5°C and scored for dauer larvae after 4 days. Detailed protocols for the assays, as well as RT-PCR experiments to verify knockdown, are provided in the Supplemental Experimental Procedures.

SUPPLEMENTAL INFORMATION

Supplemental Information includes Supplemental Experimental Procedures, five figures, and five tables and can be found with this article online at http://dx.doi.org/10.1016/j.chembiol.2016.06.015.

AUTHOR CONTRIBUTIONS

Conceptualization, J.M. and E.W.; Formal Analysis, J.M., D.W.B., Y.H.S., S.F.K., H.A.T., and E.W.; Investigation, J.M., D.W.B., and Y.H.S.; Resources, H.A.T. and E.W.; Writing – Original Draft, J.M. and E.W.; Writing – Review & Editing, J.M., D.W.B., H.A.T., and E.W.; Visualization, J.M. and E.W.; Supervision, H.A.T. and E.W.; Project Administration, H.A.T. and E.W.; Funding Acquisition, H.A.T. and E.W.

ACKNOWLEDGMENTS

We thank members of the Weerapana and Tissenbaum laboratories for assistance with experiments and manuscript preparation. This work was funded by Boston College (E.W.), The Smith Family Foundation (E.W.), and NIH grant 1R01GM118431-01A1 (E.W.). H.A.T. is a William Randolph Hearst Investigator. This project was funded in part by grants from the National Institute of Aging (AG025891) to H.A.T. and an endowment from the William Randolph Hearst Foundation to H.A.T. *C. elegans* strains were provided by the Caenorhabditis Genetics Center, which is funded by the NIH Office of Research Infrastructure Programs (P40 OD010440).

Received: January 1, 2016
Revised: June 23, 2016
Accepted: June 27, 2016
Published: August 4, 2016

REFERENCES

Adam, G.C., Sorensen, E.J., and Cravatt, B.F. (2002). Chemical strategies for functional proteomics. Mol. Cell Proteomics *1*, 781–790.

Anselmi, C.V., Malovini, A., Roncarati, R., Novelli, V., Villa, F., Condorelli, G., Bellazzi, R., and Puca, A.A. (2009). Association of the FOXO3A locus with extreme longevity in a southern Italian centenarian study. Rejuvenation Res. *12*, 95–104.

Ayyadevara, S., Dandapat, A., Singh, S.P., Siegel, E.R., Shmookler Reis, R.J., Zimniak, L., and Zimniak, P. (2007). Life span and stress resistance of *Caenorhabditis elegans* are differentially affected by glutathione transferases metabolizing 4-hydroxynon-2-enal. Mech. Ageing Dev. *128*, 196–205.

Barbieri, M., Bonafe, M., Franceschi, C., and Paolisso, G. (2003). Insulin/IGF-I-signaling pathway: an evolutionarily conserved mechanism of longevity from yeast to humans. Am. J. Physiol. Endocrinol. Metab. *285*, E1064–E1071.

Barsyte, D., Lovejoy, D.A., and Lithgow, G.J. (2001). Longevity and heavy metal resistance in daf-2 and age-1 long-lived mutants of *Caenorhabditis elegans*. FASEB J. *15*, 627–634.

Bennaars-Eiden, A., Higgins, L., Hertzel, A.V., Kapphahn, R.J., Ferrington, D.A., and Bernlohr, D.A. (2002). Covalent modification of epithelial fatty acid-binding protein by 4-hydroxynonenal in vitro and in vivo. Evidence for a role in antioxidant biology. J. Biol. Chem. *277*, 50693–50702.

Bonifati, V., Rizzu, P., van Baren, M.J., Schaap, O., Breedveld, G.J., Krieger, E., Dekker, M.C., Squitieri, F., Ibanez, P., Joosse, M., et al. (2003). Mutations in the DJ-1 gene associated with autosomal recessive early-onset parkinsonism. Science *299*, 256–259.

Brejning, J., Norgaard, S., Scholer, L., Morthorst, T.H., Jakobsen, H., Lithgow, G.J., Jensen, L.T., and Olsen, A. (2014). Loss of NDG-4 extends lifespan and stress resistance in *Caenorhabditis elegans*. Aging Cell *13*, 156–164.

Bzowska, A., Kulikowska, E., and Shugar, D. (2000). Purine nucleoside phosphorylases: properties, functions, and clinical aspects. Pharmacol. Ther. *88*, 349–425.

Cornejo Castro, E.M., Waak, J., Weber, S.S., Fiesel, F.C., Oberhettinger, P., Schutz, M., Autenrieth, I.B., Springer, W., and Kahle, P.J. (2010). Parkinson's disease-associated DJ-1 modulates innate immunity signaling in *Caenorhabditis elegans*. J. Neural Transm. *117*, 599–604.

Couvertier, S.M., Zhou, Y., and Weerapana, E. (2014). Chemical-proteomic strategies to investigate cysteine posttranslational modifications. Biochim. Biophys. Acta *1844*, 2315–2330.

Curran, S.P., and Ruvkun, G. (2007). Lifespan regulation by evolutionarily conserved genes essential for viability. PLoS Genet. *3*, e56.

Deng, X., Weerapana, E., Ulanovskaya, O., Sun, F., Liang, H., Ji, Q., Ye, Y., Fu, Y., Zhou, L., Li, J., et al. (2013). Proteome-wide quantification and characterization of oxidation-sensitive cysteines in pathogenic bacteria. Cell Host Microbe *13*, 358–370.

DePina, A.S., Iser, W.B., Park, S.S., Maudsley, S., Wilson, M.A., and Wolkow, C.A. (2011). Regulation of *Caenorhabditis elegans* vitellogenesis by DAF-2/IIS through separable transcriptional and posttranscriptional mechanisms. BMC Physiol. *11*, 11.

Depuydt, G., Xie, F., Petyuk, V.A., Shanmugam, N., Smolders, A., Dhondt, I., Brewer, H.M., Camp, D.G., Smith, R.D., and Braeckman, B.P. (2013). Reduced insulin/IGF-1 signaling and dietary restriction inhibit translation but

preserve muscle mass in *Caenorhabditis elegans*. Mol. Cell Proteomics *12*, 3624–3639.

Depuydt, G., Xie, F., Petyuk, V.A., Smolders, A., Brewer, H.M., Camp, D.G., Smith, R.D., and Braeckman, B.P. (2014). LC-MS proteomics analysis of the insulin/IGF-1-deficient Caenorhabditis elegans daf-2(e1370) mutant reveals extensive restructuring of intermediary metabolism. J Proteome Res. *13*, 1938–1956.

Dong, M.Q., Venable, J.D., Au, N., Xu, T., Park, S.K., Cociorva, D., Johnson, J.R., Dillin, A., and Yates, J.R., 3rd (2007). Quantitative mass spectrometry identifies insulin signaling targets in *C. elegans*. Science *317*, 660–663.

Evans, M.J., and Cravatt, B.F. (2006). Mechanism-based profiling of enzyme families. Chem. Rev. *106*, 3279–3301.

Fischer, M., Regitz, C., Kull, R., Boll, M., and Wenzel, U. (2013). Vitellogenins increase stress resistance of *Caenorhabditis elegans* after *Photorhabdus luminescens* infection depending on the steroid-signaling pathway. Microbes Infect. *15*, 569–578.

Flachsbart, F., Caliebe, A., Kleindorp, R., Blanche, H., von Eller-Eberstein, H., Nikolaus, S., Schreiber, S., and Nebel, A. (2009). Association of FOXO3A variation with human longevity confirmed in German centenarians. Proc. Natl. Acad. Sci. USA *106*, 2700–2705.

Furuhashi, M., and Hotamisligil, G.S. (2008). Fatty acid-binding proteins: role in metabolic diseases and potential as drug targets. Nat. Rev. Drug Discov. *7*, 489–503.

Giles, N.M., Giles, G.I., and Jacob, C. (2003). Multiple roles of cysteine in biocatalysis. Biochem. Biophys. Res. Commun. *300*, 1–4.

Girard, L.R., Fiedler, T.J., Harris, T.W., Carvalho, F., Antoshechkin, I., Han, M., Sternberg, P.W., Stein, L.D., and Chalfie, M. (2007). WormBook: the online review of *Caenorhabditis elegans* biology. Nucleic Acids Res. *35*, D472–D475.

Hamilton, B., Dong, Y., Shindo, M., Liu, W., Odell, I., Ruvkun, G., and Lee, S.S. (2005). A systematic RNAi screen for longevity genes in *C. elegans*. Genes Dev. *19*, 1544–1555.

Henderson, S.T., and Johnson, T.E. (2001). daf-16 integrates developmental and environmental inputs to mediate aging in the nematode Caenorhabditis elegans. Curr. Biol. *11*, 1975–1980.

Hohoff, C., Borchers, T., Rustow, B., Spener, F., and van Tilbeurgh, H. (1999). Expression, purification, and crystal structure determination of recombinant human epidermal-type fatty acid binding protein. Biochemistry *38*, 12229–12239.

Honda, Y., and Honda, S. (1999). The daf-2 gene network for longevity regulates oxidative stress resistance and Mn-superoxide dismutase gene expression in *Caenorhabditis elegans*. FASEB J. *13*, 1385–1393.

Hoogewijs, D., Houthoofd, K., Matthijssens, F., Vandesompele, J., and Vanfleteren, J.R. (2008). Selection and validation of a set of reliable reference genes for quantitative sod gene expression analysis in *C. elegans*. BMC Mol. Biol. *9*, 9.

Hsu, A.L., Murphy, C.T., and Kenyon, C. (2003). Regulation of aging and age-related disease by DAF-16 and heat-shock factor. Science *300*, 1142–1145.

Jensen, V.L., Gallo, M., and Riddle, D.L. (2006). Targets of DAF-16 involved in *Caenorhabditis elegans* adult longevity and dauer formation. Exp. Gerontol. *41*, 922–927.

Kamath, R.S., Fraser, A.G., Dong, Y., Poulin, G., Durbin, R., Gotta, M., Kanapin, A., Le Bot, N., Moreno, S., Sohrmann, M., et al. (2003). Systematic functional analysis of the *Caenorhabditis elegans* genome using RNAi. Nature *421*, 231–237.

Kenyon, C., Chang, J., Gensch, E., Rudner, A., and Tabtiang, R. (1993). A *C. elegans* mutant that lives twice as long as wild type. Nature *366*, 461–464.

Kimura, K.D., Tissenbaum, H.A., Liu, Y., and Ruvkun, G. (1997). daf-2, an insulin receptor-like gene that regulates longevity and diapause in Caenorhabditis elegans. Science *277*, 942–946.

Kumsta, C., Thamsen, M., and Jakob, U. (2011). Effects of oxidative stress on behavior, physiology, and the redox thiol proteome of *Caenorhabditis elegans*. Antioxid. Redox Signal. *14*, 1023–1037.

Lamitina, S.T., and Strange, K. (2005). Transcriptional targets of DAF-16 insulin signaling pathway protect *C. elegans* from extreme hypertonic stress. Am. J. Physiol. Cell Physiol. *288*, C467–C474.

Lee, R.Y., Hench, J., and Ruvkun, G. (2001). Regulation of C. elegans DAF-16 and its human ortholog FKHRL1 by the daf-2 insulin-like signaling pathway. Curr. Biol. CB *11*, 1950–1957.

Lee, J.Y., Kim, C., Kim, J., and Park, C. (2013). DJR-1.2 of *Caenorhabditis elegans* is induced by DAF-16 in the dauer state. Gene *524*, 373–376.

Li, Y., Wang, W.J., Cao, H., Lu, J., Wu, C., Hu, F.Y., Guo, J., Zhao, L., Yang, F., Zhang, Y.X., et al. (2009). Genetic association of FOXO1A and FOXO3A with longevity trait in Han Chinese populations. Hum. Mol. Genet. *18*, 4897–4904.

Li, X., Matilainen, O., Jin, C., Glover-Cutter, K.M., Holmberg, C.I., and Blackwell, T.K. (2011). Specific SKN-1/Nrf stress responses to perturbations in translation elongation and proteasome activity. PLoS Genet. *7*, e1002119.

Lin, K., Hsin, H., Libina, N., and Kenyon, C. (2001). Regulation of the Caenorhabditis elegans longevity protein DAF-16 by insulin/IGF-1 and germline signaling. Nat. Genet. *28*, 139–145.

McElwee, J., Bubb, K., and Thomas, J.H. (2003). Transcriptional outputs of the *Caenorhabditis elegans* forkhead protein DAF-16. Aging Cell *2*, 111–121.

McElwee, J.J., Schuster, E., Blanc, E., Thomas, J.H., and Gems, D. (2004). Shared transcriptional signature in *Caenorhabditis elegans* dauer larvae and long-lived daf-2 mutants implicates detoxification system in longevity assurance. J. Biol. Chem. *279*, 44533–44543.

Mukhopadhyay, A., Oh, S.W., and Tissenbaum, H.A. (2006). Worming pathways to and from DAF-16/FOXO. Exp. Gerontol. *41*, 928–934.

Murphy, C.T., McCarroll, S.A., Bargmann, C.I., Fraser, A., Kamath, R.S., Ahringer, J., Li, H., and Kenyon, C. (2003). Genes that act downstream of DAF-16 to influence the lifespan of *Caenorhabditis elegans*. Nature *424*, 277–283.

Oh, S.W., Mukhopadhyay, A., Dixit, B.L., Raha, T., Green, M.R., and Tissenbaum, H.A. (2006). Identification of direct DAF-16 targets controlling longevity, metabolism and diapause by chromatin immunoprecipitation. Nat. Genet. *38*, 251–257.

Olsen, A., Vantipalli, M.C., and Lithgow, G.J. (2006). Using *Caenorhabditis elegans* as a model for aging and age-related diseases. Ann. N. Y. Acad. Sci. *1067*, 120–128.

Pace, N.J., and Weerapana, E. (2013). Diverse functional roles of reactive cysteines. ACS Chem. Biol. *8*, 283–296.

Pace, N.J., and Weerapana, E. (2014). A competitive chemical-proteomic platform to identify zinc-binding cysteines. ACS Chem. Biol. *9*, 258–265.

Plenefisch, J., Xiao, H., Mei, B., Geng, J., Komuniecki, P.R., and Komuniecki, R. (2000). Secretion of a novel class of iFABPs in nematodes: coordinate use of the *Ascaris/Caenorhabditis* model systems. Mol. Biochem. Parasitol. *105*, 223–236.

Qian, Y., Martell, J., Pace, N.J., Ballard, T.E., Johnson, D.S., and Weerapana, E. (2013). An isotopically tagged azobenzene-based cleavable linker for quantitative proteomics. Chembiochem *14*, 1410–1414.

Riddle, D.L., Blumenthal, T., Meyer, B.J., and Priess, J.R. (1997). Introduction to *C. elegans*. In *C. elegans* II, D.L. Riddle, T. Blumenthal, B.J. Meyer, and J.R. Priess, eds. (Cold Spring Harbor).

Rostovtsev, V.V., Green, L.G., Fokin, V.V., and Sharpless, K.B. (2002). A stepwise huisgen cycloaddition process: copper(I)-catalyzed regioselective "ligation" of azides and terminal alkynes. Angew. Chem. Int. Ed. Engl. *41*, 2596–2599.

Smathers, R.L., and Petersen, D.R. (2011). The human fatty acid-binding protein family: evolutionary divergences and functions. Hum. Genomics *5*, 170–191.

Smathers, R.L., Fritz, K.S., Galligan, J.J., Shearn, C.T., Reigan, P., Marks, M.J., and Petersen, D.R. (2012). Characterization of 4-HNE modified L-FABP reveals alterations in structural and functional dynamics. PLoS One *7*, e38459.

Smathers, R.L., Galligan, J.J., Shearn, C.T., Fritz, K.S., Mercer, K., Ronis, M., Orlicky, D.J., Davidson, N.O., and Petersen, D.R. (2013). Susceptibility of L-FABP-/- mice to oxidative stress in early-stage alcoholic liver. J. Lipid Res. *54*, 1335–1345.

Storch, J., and Corsico, B. (2008). The emerging functions and mechanisms of mammalian fatty acid-binding proteins. Annu. Rev. Nutr. *28*, 73–95.

Timmons, L., Court, D.L., and Fire, A. (2001). Ingestion of bacterially expressed dsRNAs can produce specific and potent genetic interference in *Caenorhabditis elegans*. Gene *263*, 103–112.

Tullet, J.M. (2015). DAF-16 target identification in *C. elegans*: past, present and future. Biogerontology *16*, 221–234.

Walker, G.A., White, T.M., McColl, G., Jenkins, N.L., Babich, S., Candido, E.P.M., Johnson, T.E., and Lithgow, G.J. (2001). Heat shock protein accumulation is upregulated in a long-lived mutant of *Caenorhabditis elegans*. J. Gerontol. A Biol. Sci. Med. Sci. *56*, B281–B287.

Walsh, C.T., Garneau-Tsodikova, S., and Gatto, G.J., Jr. (2005). Protein post-translational modifications: the chemistry of proteome diversifications. Angew. Chem. Int. Ed. Engl. *44*, 7342–7372.

Wang, W., Fridman, A., Blackledge, W., Connelly, S., Wilson, I.A., Pilz, R.B., and Boss, G.R. (2009). The phosphatidylinositol 3-kinase/akt cassette regulates purine nucleotide synthesis. J. Biol. Chem. *284*, 3521–3528.

Wang, C., Weerapana, E., Blewett, M.M., and Cravatt, B.F. (2014). A chemoproteomic platform to quantitatively map targets of lipid-derived electrophiles. Nat. Methods *11*, 79–85.

Weerapana, E., Wang, C., Simon, G.M., Richter, F., Khare, S., Dillon, M.B., Bachovchin, D.A., Mowen, K., Baker, D., and Cravatt, B.F. (2010). Quantitative reactivity profiling predicts functional cysteines in proteomes. Nature *468*, 790–795.

Willcox, B.J., Donlon, T.A., He, Q., Chen, R., Grove, J.S., Yano, K., Masaki, K.H., Willcox, D.C., Rodriguez, B., and Curb, J.D. (2008). FOXO3A genotype is strongly associated with human longevity. Proc. Natl. Acad. Sci. USA *105*, 13987–13992.

Xu, M., Joo, H.J., and Paik, Y.K. (2011). Novel functions of lipid-binding protein 5 in *Caenorhabditis elegans* fat metabolism. J. Biol. Chem. *286*, 28111–28118.

Yang, J., Gupta, V., Carroll, K.S., and Liebler, D.C. (2014). Site-specific mapping and quantification of protein S-sulphenylation in cells. Nat. Commun. *5*, 4776.

Yu, R.X., Liu, J., True, N., and Wang, W. (2008). Identification of direct target genes using joint sequence and expression likelihood with application to DAF-16. PLoS One *3*, e1821.

Yuan, Y., Kadiyala, C.S., Ching, T.T., Hakimi, P., Saha, S., Xu, H., Yuan, C., Mullangi, V., Wang, L., Fivenson, E., et al. (2012). Enhanced energy metabolism contributes to the extended life span of calorie-restricted *Caenorhabditis elegans*. J. Biol. Chem. *287*, 31414–31426.

Zarse, K., Schmeisser, S., Groth, M., Priebe, S., Beuster, G., Kuhlow, D., Guthke, R., Platzer, M., Kahn, C.R., and Ristow, M. (2012). Impaired insulin/IGF1 signaling extends life span by promoting mitochondrial L-proline catabolism to induce a transient ROS signal. Cell Metab. *15*, 451–465.

Cell Chemical Biology, Volume *23*

Supplemental Information

Global Cysteine-Reactivity Profiling during Impaired Insulin/IGF-1 Signaling in *C. elegans* Identifies Uncharacterized Mediators of Longevity

Julianne Martell, Yonghak Seo, Daniel W. Bak, Samuel F. Kingsley, Heidi A. Tissenbaum, and Eranthie Weerapana

Supplemental Information

Detailed Experimental Procedures:

C. elegans **culture for MS and RNAi experiments**

Strain Maintenance

Worm strains were grown at 15 °C on OP50 *E. coli*-seeded nematode growth medium (NGM) stock plates using standard *C. elegans* techniques[1]. The following strains were used:

daf16;daf-2**:** DR1309 *daf-16(m26) I; daf-2(e1370) III*
daf-2**:** CB1370 *daf-2(e1370) III*
daf-16**:** GR1307 *daf-16(mgDf50) I*
Wild-type: N2

Strains were provided by the CGC, which is funded by NIH Office of Research Infrastructure Programs (P40 OD010440).

Preparation of 4 day old *daf-2* and *daf-16;daf-2* worms for MS analysis

Age-synchronization of worms was done by shaking ~3000 gravid adult worms in a solution of sterile water (5.0 mL), KOH (1.0 mL, 5 M), and bleach (4.0 mL) for 5 minutes until only the eggs remained. The eggs were centrifuged for 30 seconds (4 °C, 2500 rpm), the supernatant was removed and the eggs were washed with S Medium (5 x 10 mL). The eggs were resuspended in S Medium (8 mL) and allowed to hatch overnight in a 15 °C incubator. The next day, the hatched L1 worms (~100,000) were aliquoted onto 10 NGM plates and synchronized growth began with the addition of OP50 *E. coli* (100 µL, 100 mg/mL). The worms were grown at 15 °C until the L4 larval stage where they were transferred to 25 floxuridine-containing plates (FUDR, 0.05 mg/mL) to prevent reproduction. The worms were fed OP50 (150 µL), and moved to a 25 °C incubator. The following day was counted as day 1 of adulthood and the worms were grown until they were 4 days old. Additional OP50 was added daily as needed to prevent starvation. After 4 days, the worms were washed off the plates with PBS and any remaining bacteria, eggs, larva, deceased worms, or debris was removed via sucrose gradient separation: worms were washed with 3 x 5 mL cold 0.1 M NaCl and then suspended in 2.5 mL cold 0.1 M NaCl and 2.5 mL cold 60% sucrose in water. This was spun in a 4 °C centrifuge at 3500 rpm for 5 minutes, allowing the age-synchronized worms to float on the sucrose and pelleting the unwanted debris. The worms were carefully removed, washed with 5 x 5 mL PBS, and stored at -80 °C until lysis. The worms were resuspended in 4 mL PBS, sonicated to lyse, and spun at 5000 rpm for 10 minutes to isolate the protein extracts.

Quantitative mass spectrometry analysis using isotopic azobenzene tags: reactive cysteines in *daf-2*

Click chemistry and streptavidin enrichment of probe-labeled proteins

For each MS sample, *daf-16;daf-2* worm lysates (4 x 500 µL, 2 mg/mL) in PBS were aliquoted into 1.5 mL eppendorf tubes. Two tubes were treated with the high concentration of IA-alkyne (100 µM from 100x stock) and the other two tubes treated with the low concentration of IA-alkyne (10 µM from 100x stock) for 1 hour at room temperature. The heavy azobenzene tag (Azo-H; 100 µM) and light azobenzene tag (Azo-L; 100 µM) were added to the samples treated with 100 µM IA-alkyne and 10 µM IA-alkyne, respectively, and conjugated through click chemistry by the addition TCEP (1.0 mM from fresh 50X stock in water), ligand (100 µM from 17X stock in DMSO:t-Butanol 1:4) and $CuSO_4$ (1.0 mM from 50X stock in water). Samples were allowed to react at room temperature for 1 hour. The tubes

were combined pairwise, centrifuged for 10 minutes (5,900 g at 4 °C) to pellet the precipitated proteins, and resuspended in cold MeOH (500 µL) by sonication. The tubes were again combined pairwise, centrifuged, and washed in MeOH, after which the pellet was solubilized in PBS containing 1.2% SDS via sonication and heating (5 min, 80°C). The SDS-solubilized, probe-labeled proteome samples were diluted with PBS (5 mL) for a final SDS concentration of 0.2%. The solutions were incubated with 100 µL streptavidin-agarose beads (Thermo Scientific) at 4 °C for 16 hrs. The solutions were then incubated at room temperature for 3 hrs. The beads were washed with 0.2% SDS/PBS (5 mL) for 10 mins, PBS (3 x 5 mL), and water (3 x 5 mL). The beads were pelleted by centrifugation (1400 g, 3 mins) between washes.

On-bead trypsin digestion and azobenzene cleavage

The washed beads were suspended in 6 M urea/PBS (500 µL) and 10 mM dithiothreitol (DTT) (from 20X stock in water) and placed in a 65 °C heat block for 15 mins. Iodoacetamide (20 mM, from 50X stock in water) was then added and the samples were placed in a 37 °C incubator and agitated for 30 mins. Following reduction and alkylation, the beads were pelleted by centrifugation (1400 g, 3 min) and resuspended in 200 µL of 2 M urea/PBS, 1 mM CaCl2 (from 100X stock in water), and trypsin (2 µg). The digestion was allowed to proceed overnight at 37 °C. The digested peptides were separated from the beads using a Micro Bio-Spin column (BioRad). The beads were washed with PBS (3 x 500 µL) and water (3 x 500 µL) and subsequently transferred to screw-cap eppendorf tubes. The azobenzene cleavage was carried out by incubating the beads with 50 µL of fresh sodium dithionite in PBS (25 mM) for 1 hour at room temperature on a rotator. After centrifugation, the supernatant was transferred to a new eppendorf tube. The cleavage process was repeated twice more with 75 µL of 25 mM dithionite solution and 75 µL of 50 mM dithionite solution to ensure completion, each time combining the supernatants in the eppendorf. The beads were additionally washed twice with water (75 µL). Formic acid (17.5 µL) was added to the samples and stored at -20 °C until mass spectrometry analysis.

Liquid chromatography-mass spectrometry (LC-MS/MS)

LC-MS/MS analysis was performed on an LTQ-Orbitrap Discovery mass spectrometer (ThermoFisher) coupled to an Agilent 1200 series HPLC. Peptide digests were pressure loaded onto a 250 µm fused silica desalting column packed with 4 cm of Aqua C18 reverse phase resin (Phenomenex). The peptides were then eluted onto a biphasic column (100 µm fused silica with a 5 µm tip, packed with 10 cm C18 and 3 cm Partisphere strong cation exchange resin (SCX, Whatman)) using a gradient 5-100% Buffer B in Buffer A (Buffer A: 95% water, 5% acetonitrile, 0.1% formic acid; Buffer B: 20% water, 80% acetonitrile, 0.1% formic acid). The peptides were then eluted from the SCX onto the C18 resin and into the mass spectrometer using four salt steps as previously described[2]. The flow rate through the column was set to ~0.25 µL/min and the spray voltage was set to 2.75 kV. One full MS scan (FTMS) (400-1800 MW) was followed by 18 data dependent scans (ITMS) of the n^{th} most intense ions with dynamic exclusion disabled.

MS data analysis - peptide identification

The generated tandem MS data were searched using the SEQUEST algorithm[3] against the Uniprot *C. elegans* database. A static modification of +57.02146 on cysteine was specified to account for alkylation by iodoacetamide and differential modifications of +443.2897 (Azo-L tag) and +449.3035 (Azo-H tag) were specified on cysteine to account for probe modifications. SEQUEST output files were filtered using DTASelect2.0.5 and quantification of light:heavy ratios was performed using the CIMAGE quantification package as previously described[4].

Quantitative mass spectrometry analysis using isotopic azobenzene tags: *daf-2* vs. *daf-16;daf-2*

For each MS sample, *daf-2* and *daf-16;daf-2* worms lysates (2 x 500 µL, 2 mg/mL each) were aliquoted into 1.5 mL eppendorf tubes. The tubes were treated with IA-alkyne (100 µM from 100x stock) for 1

hour at room temperature. The Azo-H (100 μM) was added to the *daf-16;daf-2* lysates, and the Azo-L (100 μM) was added to the *daf-2* lysates and conjugated through click chemistry for 1 hour at room temperature. The rest of the procedure is the same as described above.

RNAi-mediated knockdown experiments

RNAi bacterial culture and RNAi feeding plate preparation

RNAi bacterial clones came from the Ahringer Lab RNAi feeding library (provided by the Tissenbaum Lab), which uses the L4440 vector containing T7 promoters and the TetR gene transformed into HT115 (DE3), an RNase III-deficient *E. coli* strain with IPTG-inducible T7 polymerase activity and ampicillin resistance[5]. Frozen stocks from the library were streaked on LB agar plates containing ampicillin (100 μg/mL) and tetracycline (12.5 μg/mL) and grown overnight at 37 °C. Single colonies were inoculated and used to make frozen glycerol stocks from which all RNAi plates were made. Frozen stocks were grown overnight at 37 °C in LB media (3.0 mL) with ampicillin and tetracycline. The overnight cultures (200 μL) were added to LB media (20 mL) with ampicillin only and grown for 6 hours at 37 °C. RNAi plates containing ampicillin and IPTG (1.0 mM) were seeded with this RNAi bacterial culture (~800 μL) and allowed to dry overnight in the dark. RNAi plates used for lifespan assays also contained floxuridine (FUDR, 0.1 mg/mL).

Lifespan assays

Worms were cultured for two generations on RNAi plates at 15 °C. For each lifespan assay, 30 second generation L4 worms were transferred to a new RNAi plates (with FUDR) and moved to 20 °C. After 7 days, the worms were censored for “sick” phenotypes (e.g. vulva bursting) and then scored by gently tapping with a platinum wire every 2-3 days. Worms that crawled off the plate or into mold that was excised out of the agar were censored from the analysis. Four replicates of each plate were performed.

Dauer formation assays

daf-2 worms were cultured for two generations on RNAi plates at 15 °C. For each dauer formation assay, 9 second generation L4 worms from each RNAi plate were transferred to 3 new RNAi plates and allowed to lay eggs overnight. The next day, adult worms were removed from the plates and the remaining eggs were moved to a 22.5 °C incubator. After 4 days, the worms were scored for dauer larva and the percentage of dauer larva was compared to L4440 vector-treated *daf-2* control worms. Several temperatures between 20-25 °C were tested to determine which was most appropriate to cause 10-20% dauer arrest in the control worms (not shown).

Evaluation of mRNA levels in L4440 vector- and RNAi-treated *C. elegans*

RNA Extraction

Worms grown on RNAi plates were removed via washing with DEPC-water into an RNAse-free 1.5 mL eppendorf tube. After the worms were allowed to settle, the supernatant was removed and the worms were washed with 1 mL of DEPC-water and rotated at room temperature for 20 minutes to remove excess RNAi bacteria. This washing step was repeated 4 more times. Excess DEPC-water was removed and TRIzol reagent (1.0 mL) was added, briefly agitated, and allowed to incubate at room temperature for 5 minutes. Chloroform (200 μL) was added to the tube, inverted to mix, let sit at room temperature for 3 minutes, and centrifuged for 15 minutes at 4 °C. The top layer was carefully transferred to another eppendorf tube and isopropanol (400 μL) added, vortexed well, and allowed to sit at room temperature for 10 minutes. The tube was centrifuged for 10 minutes at 4 °C and the supernatant was removed, leaving a white pellet which was then washed with a 75% EtOH in DEPC-water solution (200 μL). The tube was centrifuged for 5 minutes at 4 °C, the supernatant was removed, and the RNA pellet was allowed to air dry for ~10 minutes. The pellet was resuspended in DEPC-water (20-30 μL) and RNA concentrations were determined using the Nanodrop.

cDNA formation

RNA stocks were diluted to 500 ng/µL. DEPC-water (9.5 µL), RNA (1.0 µL, 500 ng/µL = 500 ng), and Oligo-dT's (2.0 µL, 100 µM) were combined in an RNAse-free PCR tube. The tube was incubated at 65 °C for 2 minutes and then chilled on ice for 1 minute. M MuLV Reverse Transcriptase 10x Reaction Buffer (2.0 µL), dNTP mix (2.0 µL, 10 mM), DTT (2.0 µL, 100 mM), RNAse Inhibitor (0.5 µL), and M MuLV Reverse Transcriptase (1.0 µL) were added to the sample giving a total volume of 20.0 µL. The tubes were briefly mixed and then incubated at 37 °C for 60 minutes, then 85 °C for 5 minutes to terminate the reaction. The tubes were allowed to sit on ice for 1 minute, and stored at -80 °C.

RT-PCR

The following primers were designed to evaluate LBP-3, K02D7.1, and PMP-3 mRNA levels. PMP-3 was used a control because of its unusually stable expression levels, with little variation between adults, dauer, and L3 larvae, or between wild-type and *daf-2* or *daf-16* mutants. For each gene, the primers were prepared as a mixture of both the forward and reverse primer (10uM each) in DEPC-water.

lbp-3 forward**:** 5'**-**GCTGCTAAAGGAGTGAGCT-3'
lbp-3 reverse**:** 5'**-**CCATTGTTGACCATTTTCATGAC-3'

pmp-3 forward**:** 5'**-**GGCTAACTTATGAAAGTTCCG-3'
pmp-3 reverse**:** 5'**-**GATGAGTGACTCCAGCAAGT-3'

K02D7.1 forward**:** 5'**-**CAATTCACCAACCAACGCTG-3'
K02D7.1 reverse**:** 5'**-**TGAACCGATACAAATCGGGC-3'

For each sample, DEPC-water (16.8 µL), 5x HF Buffer (5.0 µL), primer mix (1.50 µL), cDNA (1.0 µL), dNTPs (0.5 µL, 10 mM), and Phusion polymerase (0.25 µL). The following PCR conditions were used:

	30 cycles				
Initial	Denature	Anneal	Elongation	Final	
95 °C	95 °C	55 °C	68 °C	72 °C	4 °C
2 mins	15 sec	30 sec	30 sec	10 mins	End

Xylene cyanol (5.0 µL) was added to the samples and each sample (5.0 µL) and the Tri-Dye 100 bp DNA ladder were loaded onto a 2% agarose gel. The gel was run at 155 volts for 15 mins and then visualized under UV light.

References

1. Stiernagle, T., Maintenance of C. elegans. *WormBook : the online review of C. elegans biology* **2006**, 1-11.

2. Weerapana, E.; Speers, A. E.; Cravatt, B. F., Tandem orthogonal proteolysis-activity-based protein profiling (TOP-ABPP)--a general method for mapping sites of probe modification in proteomes. *Nature protocols* **2007,** *2* (6), 1414-25.

3. Eng, J. K.; McCormack, A. L.; Yates, J. R., An approach to correlate tandem mass spectral data of peptides with amino acid sequences in a protein database. *Journal of the American Society for Mass Spectrometry* **1994,** *5* (11), 976-89.

4. Weerapana, E.; Wang, C.; Simon, G. M.; Richter, F.; Khare, S.; Dillon, M. B.; Bachovchin, D. A.; Mowen, K.; Baker, D.; Cravatt, B. F., Quantitative reactivity profiling predicts functional cysteines in proteomes. *Nature* **2010,** *468* (7325), 790-5.

5. (a) Timmons, L.; Court, D. L.; Fire, A., Ingestion of bacterially expressed dsRNAs can produce specific and potent genetic interference in Caenorhabditis elegans. *Gene* **2001,** *263* (1-2), 103-12; (b) Timmons, L.; Fire, A., Specific interference by ingested dsRNA. *Nature* **1998,** *395* (6705), 854.

Supplemental Figures

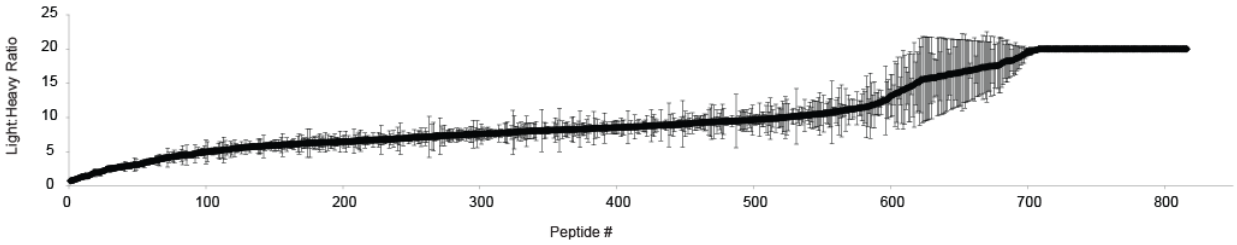

Figure S1. Related to Figure 1 and Table S1. Cysteine reactivity profiling in *C. elegans*. Average heavy:light ratios (R) are shown for 816 cysteine residues identified in four replicates of *daf-16;daf-2* lysates treated with either 10 μM (heavy) or 100 μM (light) IA (Table S1). Error bars represent standard deviation from the mean across the four replicate analyses.

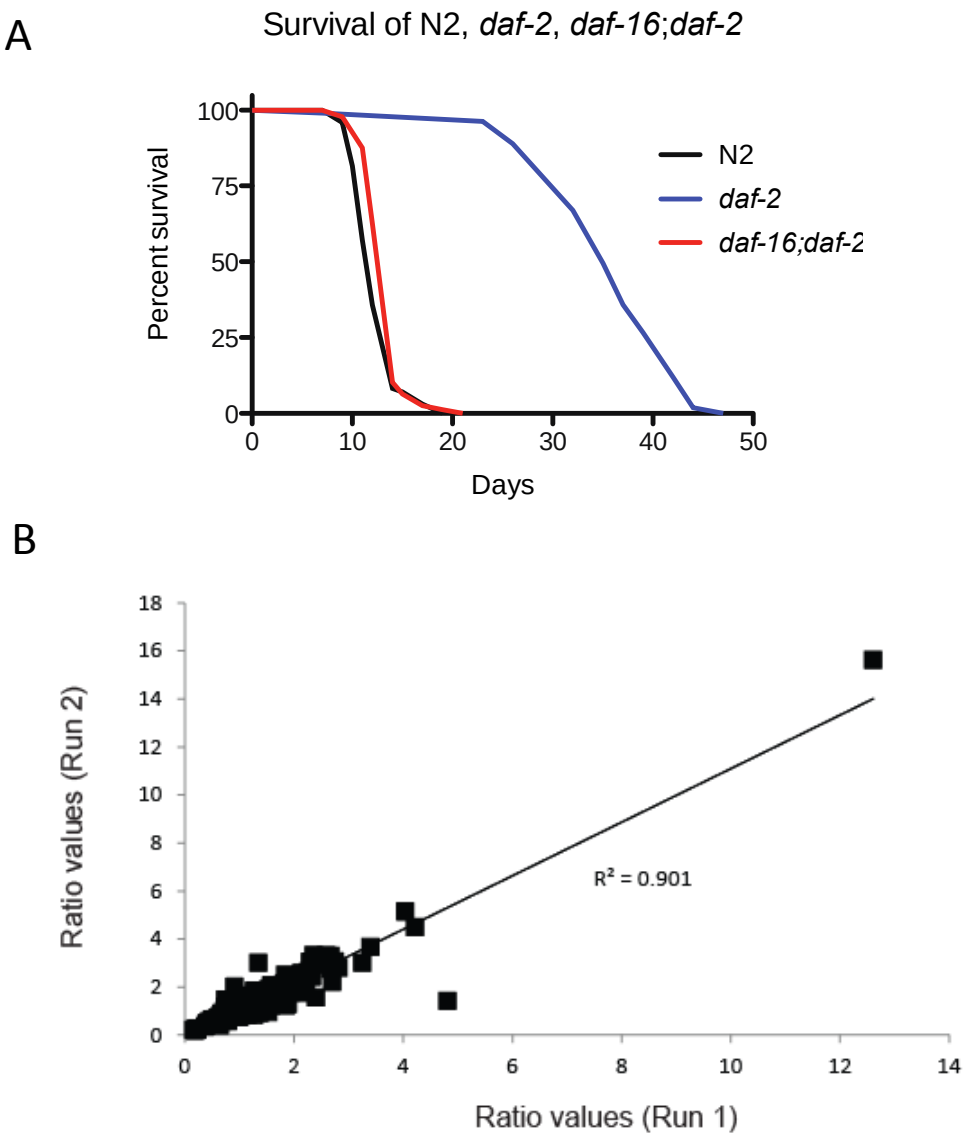

Figure S2. Related to Figure 2 and Table S2. Comparing *daf-2* and *daf-16;daf-2* mutants. (A) Lifespan assays of wild type (N2), *daf-2* and *daf-16;daf-2* mutants. Data obtained from lifespan assays to confirm that *daf-2* mutants show a ~2-fold extension in lifespan relative to *daf-16;daf-2* and N2. (B) Comparing cysteine reactivity in *daf-2* and *daf-16;daf-2* mutants. Correlation of light:heavy ratio (R) values obtained for 338 peptides in two replicates.

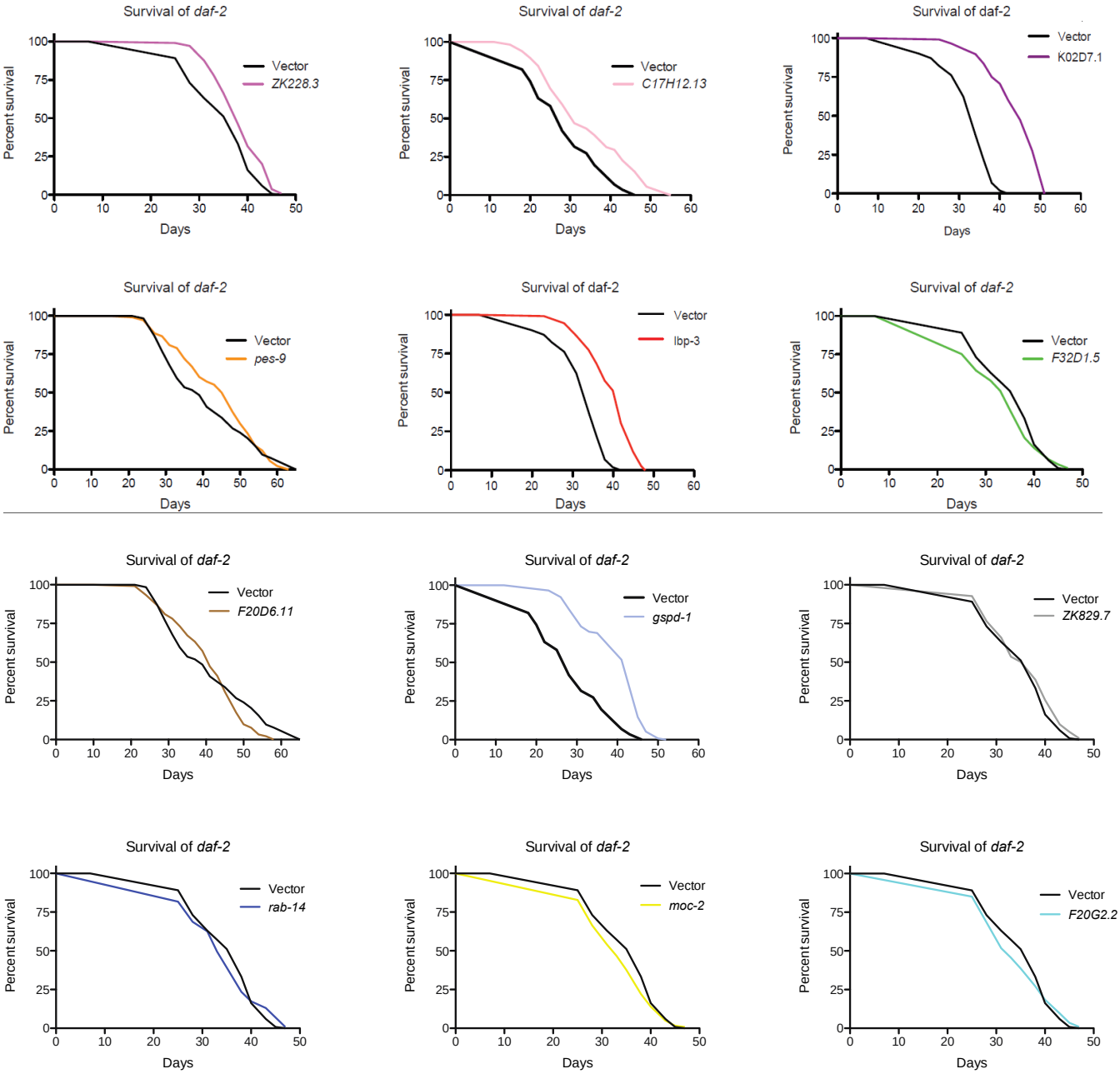

Figure S3. Related to Figure 3. RNAi and lifespan assays. Lifespan assays on RNAi-mediated knockdown of cysteine-containing proteins with the greatest reactivity change between *daf-2* and *daf-16;daf-2* worms. Out of the top 20 proteins with the greatest changes (10 increase, 10 decrease) the Ahringer RNAi library had bacterial strains available to target 17 of them. The 12 proteins with no previous information on the effects their RNAi-mediated knockdown has on longevity were chosen for our lifespan assays.

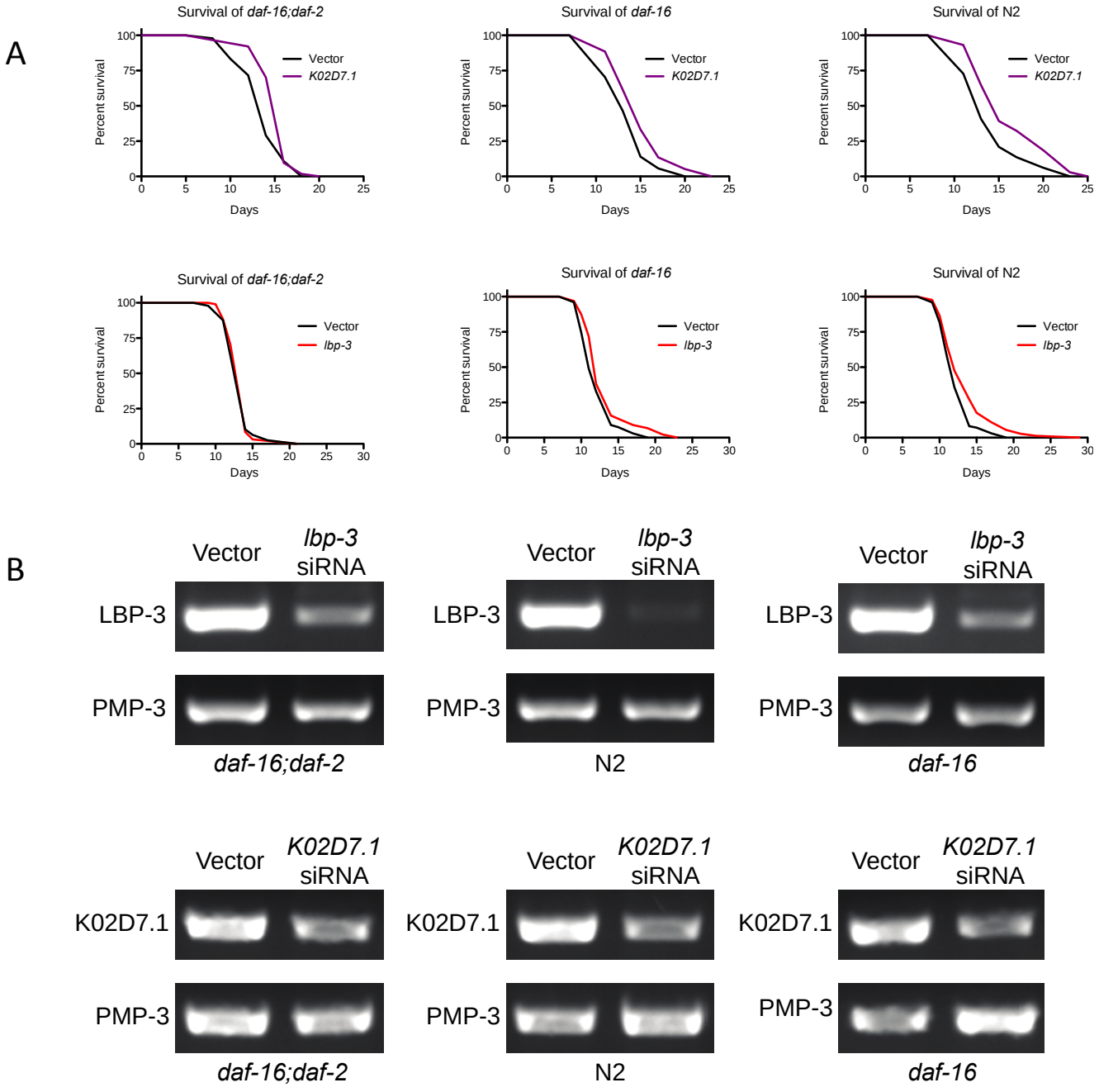

Figure S4. Related to Figure 3. RNAi studies on *lbp-3* and *K02D7.1.* (A) Lifespan assays of RNAi-mediated knockdown of *lbp-3* and *K02D7.1* in the background of *daf-16* mutants, *daf-16;daf-2* double mutants, and wild type (N2) worms. (B) RT-PCR of *daf-16* mutants, *daf-16;daf-2* double mutants, and wild type (N2) worms treated with *lbp-3* or *K02D7.1* siRNA using primers for *lbp-3*, *K02D7.1*, or *pmp-3* as a control.

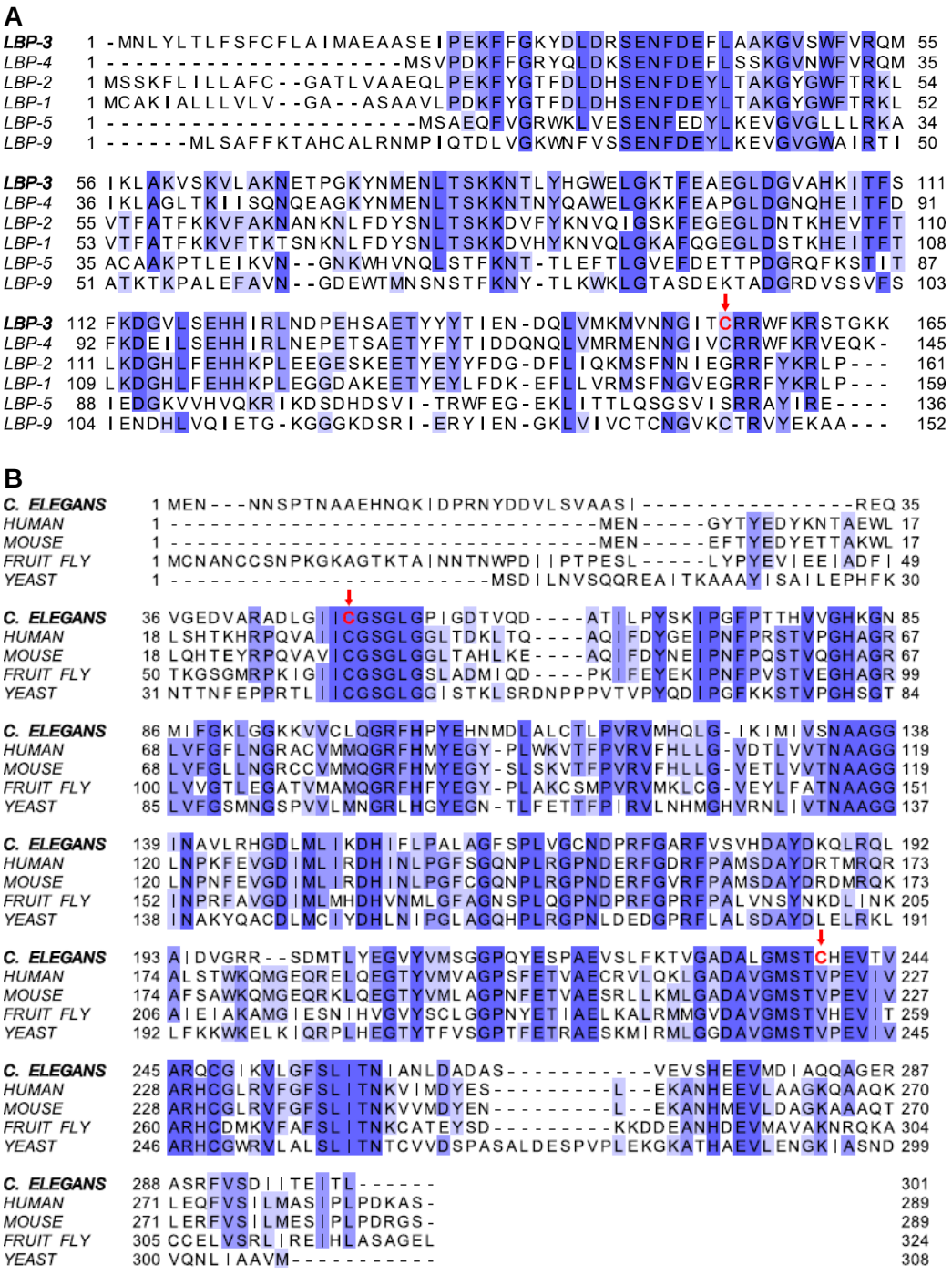

Figure S5. Related to Figure 3. LBP-3 and K02D7.1 (A) Alignment of *C. elegans* LBP-3 with the human FABP family. The reactive cysteine identified in proteomic studies is highlighted in red. (B) Alignment of *C. elegans* K02D7.1 with purine nucleoside phosphorylases from other species. The reactive cysteines identified in proteomic studies are highlighted in red.

Supplemental Tables

Table S1. Related to Figure 1. (attached as an excel file) Cysteine reactivity data. MS analysis showing the 816 cysteine-containing peptides identified in the *daf-16;daf-2* lysates treated with either 10 or 100 μM IA. The cysteines are ranked by reactivity based on their average light:heavy ratio; lower ratios indicate higher reactivity. Identified cysteines with an annotated biological function in *C. elegans* are shown. The closest human homologue for each cysteine-containing protein was determined by performing a BLAST search against the human UniProt database and functional cysteines that are conserved between *C. elegans* and humans are shown. Conservation of the cysteine residue across five species (human, mouse, fly, yeast, mustard) are shown.

Table S2. Related to Figure 2. (attached as an excel file) Comparing *daf-2* and *daf-16;daf-2* lysates. MS analysis showing the 338 cysteine-containing peptides identified in *daf-2* and *daf-16;daf-2* lysates, in order from average light:heavy ratios of < 1 (decreased cysteine reactivity in *daf-2*) to > 1 (increased cysteine reactivity in *daf-2*). All cysteines shown on this table were identified in both biological replicates. Any cysteine with an annotated biological function in *C. elegans* is shown. The closest human homologue for each cysteine-containing protein was determined by performing a BLAST search against the human UniProt database and functional cysteines that are conserved between *C. elegans* and humans are shown. Conservation of the cysteine residue across five species (human, mouse, fly, yeast, mustard) are shown.

Table S3. Related to Figure 2. (attached as an excel file) Comparison to previous redox-proteomics study. Comparison of proteins and cysteines identified in this study to a redox-proteomics study (Kumsta, C., Thamsen, M., and Jakob, U. (2011). Effects of oxidative stress on behavior, physiology, and the redox thiol proteome of Caenorhabditis elegans. Antioxid Redox Signal *14*, 1023-1037). “x” indicates that the cysteine was identified to be oxidized in the Kumsta et al. redox proteomics study.

Table S4. Related to Figure 3. Lifespan and dauer assay data. RNAi was performed on the 12 genes listed and lifespan assays were conducted on all 12 RNAi worms. Median lifespan and % change relative to the corresponding vector control were calculated for each RNAi worm. Please note that these lifespan assays were run in batches, and the vector control showed different median lifespans between batches due to slight variations in growth temperature. For each RNAi worm population the % change in lifespan was calculated based on a vector control cultured within that same batch. All lifespan data was performed as four biological replicates (see detailed data for *lbp-3* and *K02D7.1* in Table S5). RNAi knockdown worms that showed a >15% change in lifespan (*K02D7.1*, *pes-9*, *lbp-3* and *gspd-1*) were subjected to dauer assays and the % change in dauer formation was compared to the corresponding vector control. As before, dauer assays were performed in individual batches resulting in differences between the vector controls. Each RNAi population was compared to the vector control within that batch for determining the % change. Dauer assays were run as three biological replicates.

	Gene	**Median Lifespan**			**Dauer Formation**		
		RNAi	***Vector***	***Change***	***RNAi***	***Vector***	***Change***
Decrease in daf-2	*ZK228.3*	37.4	35.2	6.34%	-	-	-
	C17H12.13	30.3	26.5	14.2%	-	-	-
	K02D7.1	44.4	32.5	36.6%	48.0%	16.4%	31.6%
	pes-9	45.0	38.1	18.3%	24.8%	31.6%	-6.80%
	lbp-3	40.1	32.5	23.4%	29.7%	16.4%	13.3%
	F32D1.5	33.2	35.2	-5.67%	-	-	-
Increase in daf-2	*F20D6.11*	40.4	38.1	6.2%	-	-	-
	gspd-1	41.2	26.5	55.4%	46.3	83.6%	-37.3%
	ZK829.7	35.1	35.2	-0.40%	-	-	-
	Rab-14	32.9	35.2	-6.43%	-	-	-
	Moc-2	32.1	35.2	-8.77%	-	-	-
	F20G2.2	31.6	35.2	-10.3%	-	-	-

Table S5. Related to Figure 3. (attached as an excel file) Lifespan data for *lbp-3* and *K02D7.1* RNAi worms. Data for the number of worms alive on *lbp-3* and *K02D7.1* RNAi plates in each of four replicates for the lifespan assays. Also shown are values for average lifespan of RNAi and vector controls and calculated p-values showing significance.